



Contents lists available at ScienceDirect

## Arabian Journal of Chemistry

journal homepage: [www.ksu.edu.sa](http://www.ksu.edu.sa)

Original article

# Magnetic covalent organic framework with ionic tags as an efficient catalyst in the preparation of 2,3-disubstituted thiazolidine-4-ones and *N*-amino-2-pyridones

Erfan Abdoli, Morteza Torabi, Meysam Yarie\*, Mohammad Ali Zolfigol\*

Department of Organic Chemistry, Faculty of Chemistry and Petroleum Sciences, Bu-Ali Sina University, Hamedan, Iran



## ARTICLE INFO

## Keywords:

Covalent organic framework  
Heterogeneous catalyst  
*N*-amino-2-pyridones Thiazolidine-4-one

## ABSTRACT

The functionalization of magnetic nanoparticles with covalent organic frameworks (COFs) will endow them inspiring characteristics. Herein, a new magnetic covalent organic framework (MCOF) decorated with trifluoroacetate as ionic sections ( $\text{Fe}_3\text{O}_4@ \text{COF-TFA}$ ) was designed and constructed. To confirm the successful synthesis of this hybrid material, several techniques including Fourier-transform infrared spectroscopy (FT-IR), thermogravimetric analysis (TGA), derivative thermogravimetry (DTG), field-emission scanning electron microscopy (FE-SEM), energy-dispersive X-ray spectroscopy (EDS), elemental mapping, transmission electron microscopy (TEM), vibrating-sample magnetometer (VSM) and X-ray diffraction analysis (XRD) were applied. TG/DTG analyses show that  $\text{Fe}_3\text{O}_4@ \text{COF-TFA}$  has an excellent thermal stability up to 450 °C. The FE-SEM analysis revealed that catalyst has the island-like morphology and according to TEM analysis, it has spherical geometry with nanometer scale particle size. Also, surface area of  $\text{Fe}_3\text{O}_4@ \text{COF}$  and  $\text{Fe}_3\text{O}_4@ \text{COF-TFA}$  are 74 and 12  $\text{m}^2 \cdot \text{g}^{-1}$ , respectively.  $\text{Fe}_3\text{O}_4@ \text{COF-TFA}$  was applied as a recoverable heterogeneous catalyst for construction of 2,3-disubstituted thiazolidine-4-ones and *N*-amino-2-pyridones via a multi-component synthetic strategy. It is worth mentioning that synthesized derivatives have a good yield and short reaction times.

## 1. Introduction

Since the emergence of COFs as strong covalently linked two- and three-dimensional organic structures, these versatile materials have attracted considerable interest (Waller et al., 2015; Kandambeth et al., 2018). These reticular, sustainable as well as environmentally gentle materials possess unique properties such as high thermal and chemical stability, regulatable physicochemical characteristics, metal-free and flexible scaffolds, extremely low density, high surface area, tolerable charge-carrier mobility, and large pore sizes (Bayatani et al., 2023; Tan et al., 2023; Geng et al., 2020). COFs have been profoundly deliberated in electronics (Yang and Börjesson, 2022), energy storage (Cao et al., 2019), solar cells (Wu et al., 2018), gas capture and separation (Abdoli, 2023), water treatment (Wang et al., 2020), self-healing materials (Zhang et al., 2022), catalysis (Yusran et al., 2020) and drug delivery (Bai et al., 2016). In recent years, COFs have been enormously applied in many catalytic transformations (Guo and Jiang, 2020; Yarie, 2021; Torabi, 2021). These materials due to intrinsic catalytic activities, well-defined active sites, designability and excellent stability have a robust

partnership in catalytic and photocatalytic processes (Yang et al., 2020),  $\text{CO}_2$  fixation utility (Yang et al., 2020), multi-component reactions (Yao et al., 2021), electrocatalytic processes (Chen et al., 2022) and coupling reactions (Qiu et al., 2020). Due to the easy post-modification of COFs by active metallic groups, acidic or basic moieties and ionic sections, it is possible to design robust catalytic systems in a targeted approach (Gao et al., 2019; Segura et al., 2019). Also, to address the limitations of COFs and improve their catalytic activity, these compounds can be designed as hybrid composites by incorporation of magnetic nanoparticles, graphene oxides, carbon nanotubes, MXenes and MOFs (Zhuang and Wang, 2021; Zhao et al., 2021; Wang et al., 2022; Cai et al., 2019).

In the last years, the development, and applications of magnetic nanoparticles (MNPs) have been the subject of intensive research by many industrial and academic researchers. They have motivated them to focus on synthetic routes and extraordinary as well as vast applications of MNPs (Ma et al., 2021; Mokhtary, 2016). The lucrative utilities of MNPs in medicine, biosensing, agriculture, drug delivery and catalytic processes is undeniable (Zandipak and Sobhanardakani, 2018; Sobhanardakani et al., 2018). MNPs due to their high thermal and chemical

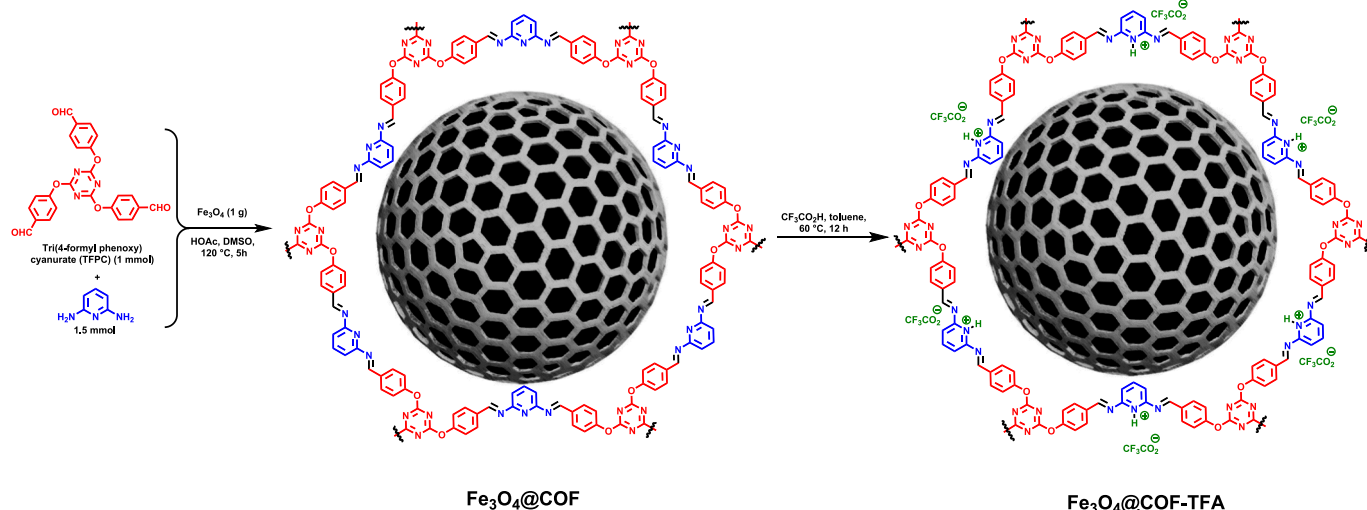
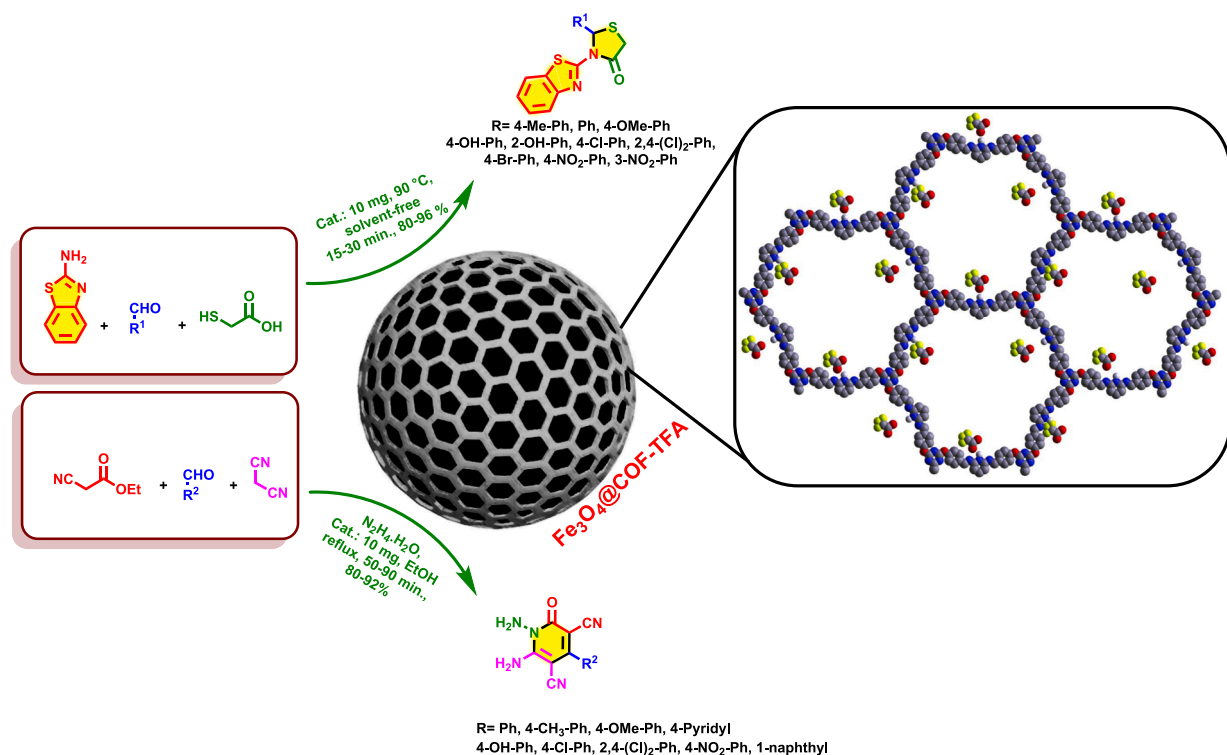
\* Corresponding authors.

E-mail addresses: [myarie.5266@gmail.com](mailto:myarie.5266@gmail.com), [m.yarie92@basu.ac.ir](mailto:m.yarie92@basu.ac.ir) (M. Yarie), [zolfi@basu.ac.ir](mailto:zolfi@basu.ac.ir), [mzolfigol@yahoo.com](mailto:mzolfigol@yahoo.com) (M. Ali Zolfigol).<https://doi.org/10.1016/j.arabjc.2024.105908>

Received 22 February 2024; Accepted 30 June 2024

Available online 15 July 2024

1878-5352/© 2024 The Authors. Published by Elsevier B.V. on behalf of King Saud University. This is an open access article under the CC BY-NC-ND license (<http://creativecommons.org/licenses/by-nc-nd/4.0/>).

Scheme 1. Synthesis of Fe<sub>3</sub>O<sub>4</sub>@COF and Fe<sub>3</sub>O<sub>4</sub>@COF-TFA.Scheme 2. General route for the catalytic preparation of thiazolidine-4-ones and *N*-amino-2-pyridones.

stability, ease of separation and reuse, high specific surface area, cheap and accessible as well as environmentally friendly nature are constantly gaining much attention (Gloag et al., 2019). Due to the excellent performance of MNPs, these compounds have found their position as an integral part of new sciences and appear as hybrid systems with other useful chemical compounds such as MOFs, COFs, DESs, etc. (Zhao et al., 2019; Torabi et al., 2022; Torabi et al., 2020; Zhuang et al., 2020; Govan and Gun'ko, 2014). Hence, these materials have represented good catalytic applications in many organic reactions such as multi-component (Torabi et al., 2021), oxidation/reduction (Payra et al., 2017), coupling (Shaikh and Zahir, 2022), asymmetric synthesis (Primitivo et al., 2021) and protection processes (Khaef et al., 2020).

Recently, the incorporation of MNPs within the COFs to achieve unique heterogeneous catalytic systems has received the attention of

chemists and their emphasis. (Sharma et al., 2020). On the other hand, modification of heterogeneous catalysts by ionic liquids can enhance their catalytic utilities (Ghasemi et al., 2020). Due to the fruitful performance of ionic liquids in catalytic transformations, there are several reports regarding MNPs, or COFs decorated by ionic liquid. Therefore, the functionalization of MNPs-COF hybrids by ionic sections deserves more attention because it can open a new window to the world of catalysis (Anizadeh et al., 2022; Chen et al., 2021; Alishahi et al., 2023).

According to the literatures, 2-pyridone containing heterocycles have a brilliant background in many areas such as functional materials, organic dyes, agricultural compounds, versatile synthons, biological compounds, and pharmaceutical molecules (Zarei et al., 2023; Tavassoli et al., 2023; Fujii et al., 2013). Also, 2-pyridones are widely found in natural products such as amrinone, millrinone, and ciclopirox

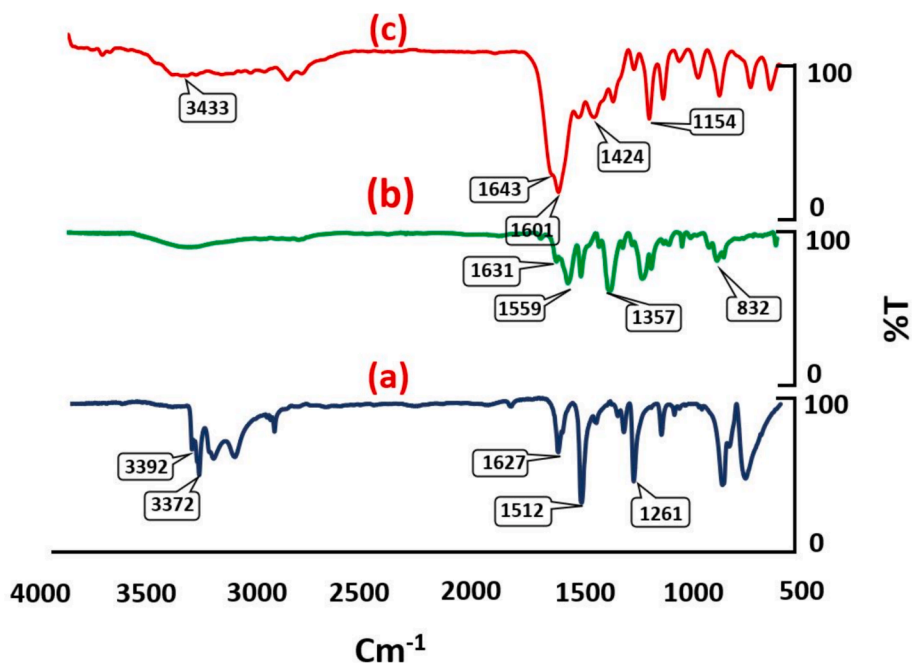


Fig. 1. (a) FT-IR spectrum of 2,6-diaminopyridine, (b) FT-IR spectrum of  $\text{Fe}_3\text{O}_4@COF$ , (c) FT-IR spectrum of  $\text{Fe}_3\text{O}_4@COF-TFA$ .

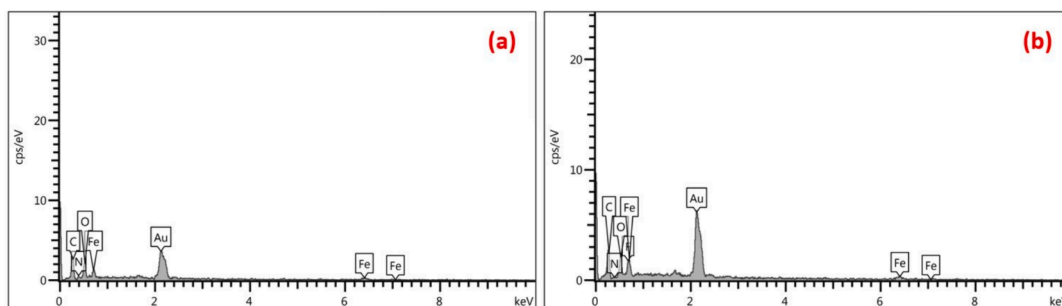


Fig. 2. EDS spectra of (a)  $\text{Fe}_3\text{O}_4@COF$  and (b)  $\text{Fe}_3\text{O}_4@COF-TFA$ .

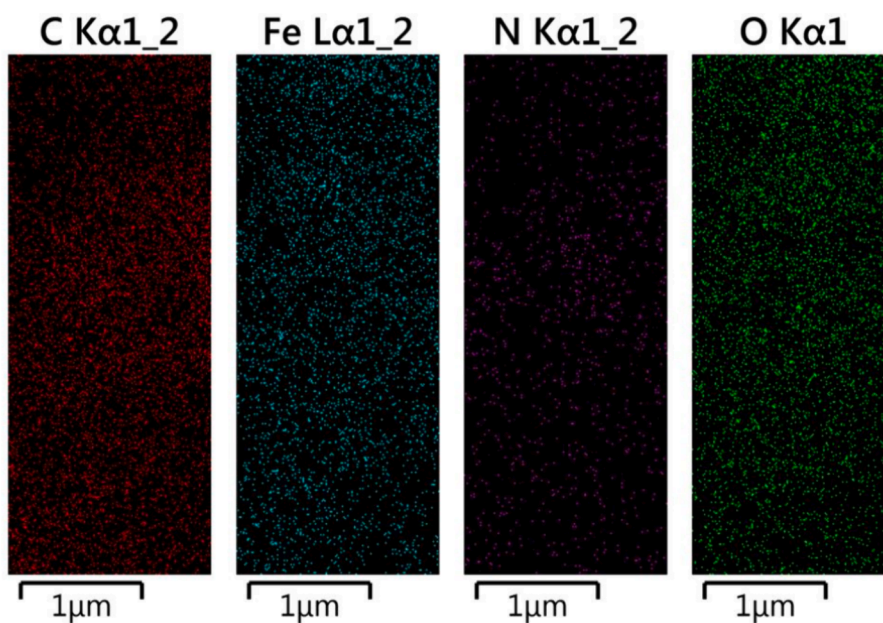


Fig. 3. Elemental distribution of  $\text{Fe}_3\text{O}_4@COF$ .

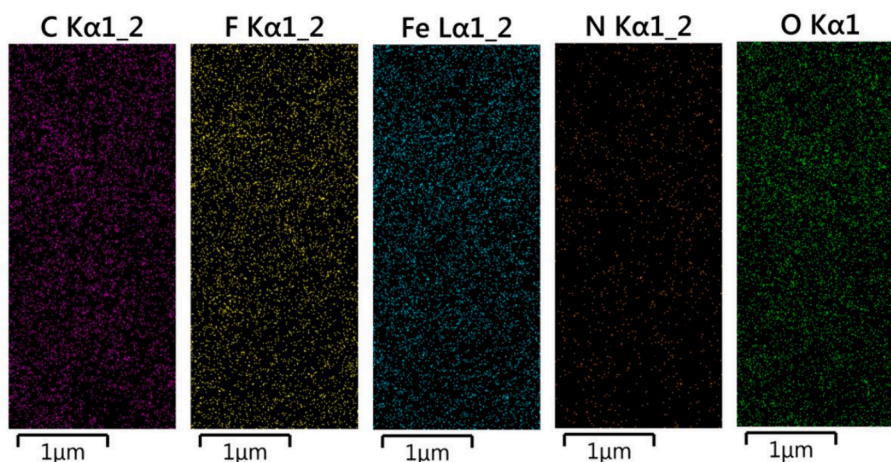


Fig. 4. Elemental distribution of  $\text{Fe}_3\text{O}_4@\text{COF-TFA}$ .

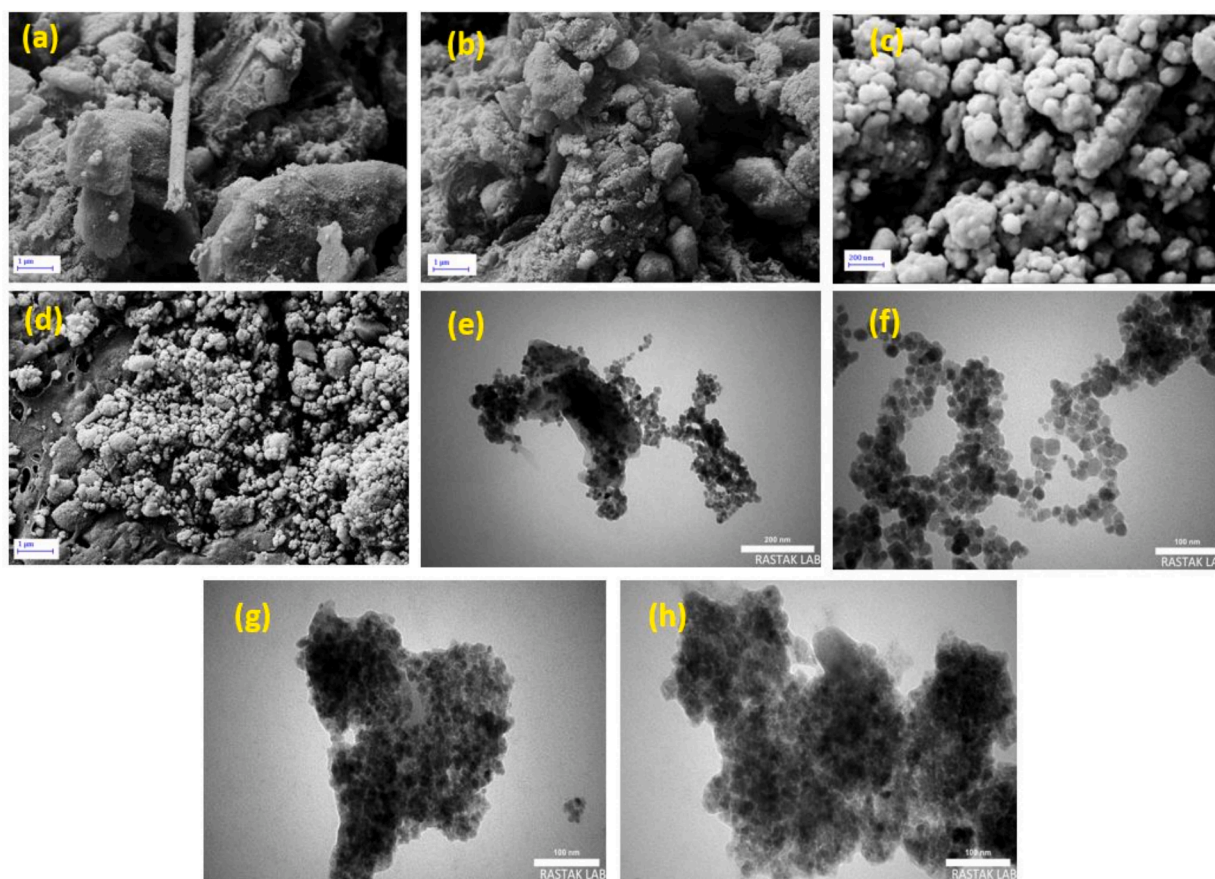


Fig. 5. FESEM images of  $\text{Fe}_3\text{O}_4@\text{COF}$  (a, b),  $\text{Fe}_3\text{O}_4@\text{COF-TFA}$  (c, d) and TEM images of  $\text{Fe}_3\text{O}_4@\text{COF}$  (e, f) and  $\text{Fe}_3\text{O}_4@\text{COF-TFA}$  (g, h).

(Hernández et al., 2013; Fossa et al., 2003). In addition, *N*-amino-2-pyridones as one of the most important families of 2-pyridone, have been widely studied by chemists. Fabulous medicinal properties such as antimicrobial (Ahadi et al., 2021), anticancer (Amer et al., 2021), anticoagulant (Babae et al., 2020), anti-HIV (Zhang et al., 2022) anti-malarial (Sangwan et al., 2022), anticonvulsant (Keshk et al., 2021), antimalarial (Hurtado-Rodríguez et al., 2022), and antihypertensive (Hernández, xxxx) have been reported for *N*-amino-2-pyridone bearing molecules.

Due to their fundamental and superior applications in vast domains of chemistry such as natural products, agricultural chemistry,

pharmaceuticals, and functional materials, thiazolidine-4-one scaffolds have gained significant importance (Tawfeek et al., 2022). However, the most important uses of thiazolidine-4-ones is their exceptional and innumerable pharmaceutical and medicinal utilities such as anticancer (Ansari et al., 2020), antioxidant (Jaiswal et al., 2019), anti-inflammatory (Jaiswal et al., 2019), cardiovascular (Jaiswal et al., 2019), antimicrobial (Jaiswal et al., 2019) and anti-HIV (Jaiswal et al., 2019). Furthermore, these compounds are well-known in hybrid drugs which are as good as marketed drugs (Khan et al., 2022).

In continuous of our research on MCOFs (Alishahi et al., 2023), we designed and synthesized a new pyridine-based MCOF decorated with

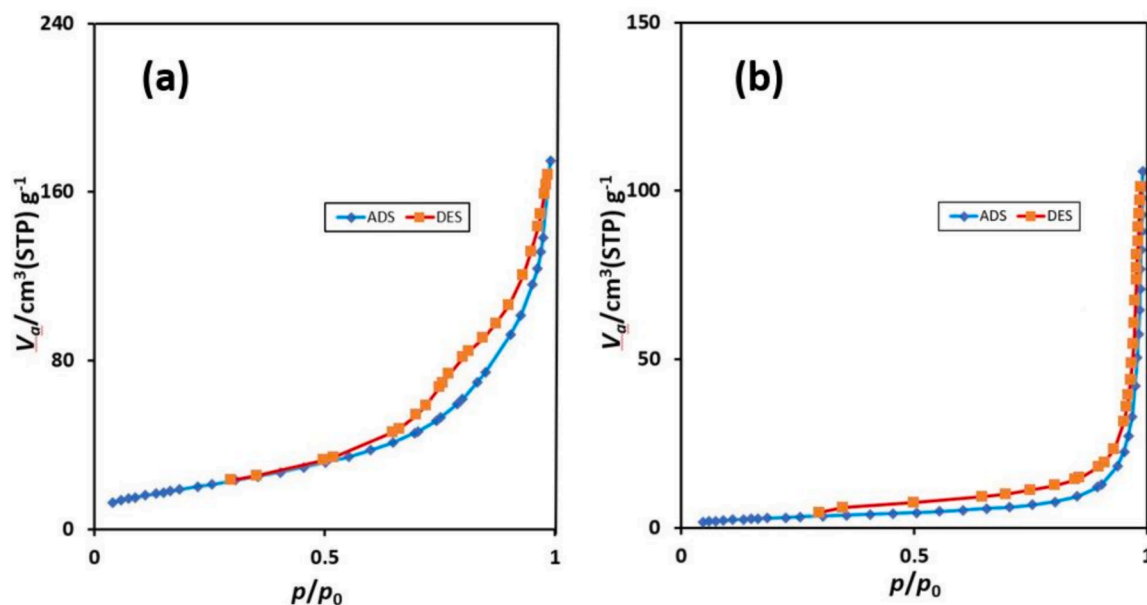


Fig. 6. Nitrogen adsorption/desorption isotherms of (a)  $\text{Fe}_3\text{O}_4@\text{COF}$  and (b)  $\text{Fe}_3\text{O}_4@\text{COF-TFA}$ .

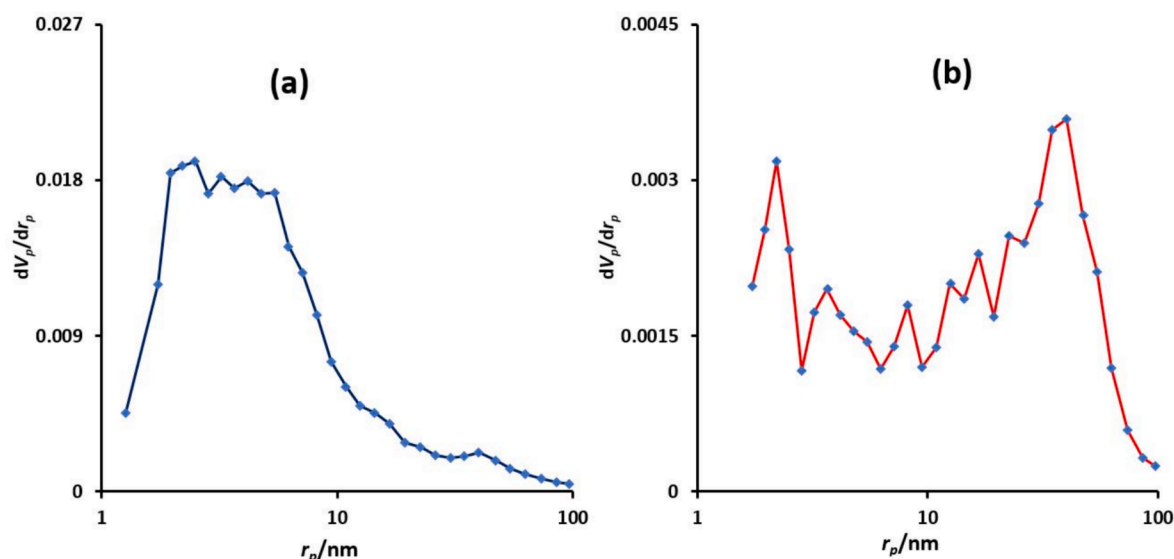


Fig. 7. Pore size distribution curves of  $\text{Fe}_3\text{O}_4@\text{COF}$  (a) and  $\text{Fe}_3\text{O}_4@\text{COF-TFA}$  (b).

trifluoroacetate as ionic sections namely  $\text{Fe}_3\text{O}_4@\text{COF-TFA}$ . After the characterization of  $\text{Fe}_3\text{O}_4@\text{COF-TFA}$ , its catalytic behavior was tested for the preparation of 2,3-disubstituted thiazolidine-4-ones and *N*-amino-2-pyridones *via* a multi-component strategy (Baharfar et al., 2019) (Scheme 1; 2).

## 2. Results and discussion

Magnetic catalysts and catalytic systems are currently attracting great attention from researchers and industries. In continuous of our previous research on MCOFs (Alishahi et al., 2023),  $\text{Fe}_3\text{O}_4@\text{COF-TFA}$  was designed, constructed and applied as a catalyst for the multi-component synthesis of thiazolidine-4-ones and *N*-amino-2-pyridones. At first, various characterization techniques were used to approve the structure, morphology, and physical properties of  $\text{Fe}_3\text{O}_4@\text{COF-TFA}$ . In continued its application in the synthesis of thiazolidine-4-ones and *N*-amino-2-pyridones was explored.

### 2.1. Characterization

Several characteristic techniques supported the proposed chemical structure of  $\text{Fe}_3\text{O}_4@\text{COF-TFA}$ . The FT-IR spectrum of tri(4-formyl phenoxy) cyanurate (TFPC) illustrates stretching vibrations characteristic of  $\text{C}=\text{O}$  at  $1701\text{ cm}^{-1}$  and the breathing mode of the triazine ring is observed at  $808\text{ cm}^{-1}$  (See ESI). Also, the FT-IR spectrum of 2,6-diaminopyridine shows the typical peaks of  $\text{NH}_2$  about at  $3372$  and  $3392\text{ cm}^{-1}$  and  $\text{C}=\text{N}$  bond (pyridine ring) at  $1627\text{ cm}^{-1}$  (Fig. 1a). The disappearance of  $\text{C}=\text{O}$  in FT-IR of TFPC and  $\text{NH}_2$  signals of 2,6-diaminopyridine as well as the appearance of a new signal about  $1631\text{ cm}^{-1}$  (imine functional group) verified the successful synthesis of  $\text{Fe}_3\text{O}_4@\text{COF}$  (Fig. 1b). Also, according to the FT-IR spectrum of  $\text{Fe}_3\text{O}_4@\text{COF-TFA}$  (Fig. 1c), the existence of broader peaks compared to the previous step confirmed the successful addition of TFA to  $\text{Fe}_3\text{O}_4@\text{COF}$ . Of note, the new peak at  $1643\text{ cm}^{-1}$  can be related to the carbonyl functional group of TFA.

EDS spectra of  $\text{Fe}_3\text{O}_4@\text{COF}$  and  $\text{Fe}_3\text{O}_4@\text{COF-TFA}$  samples were

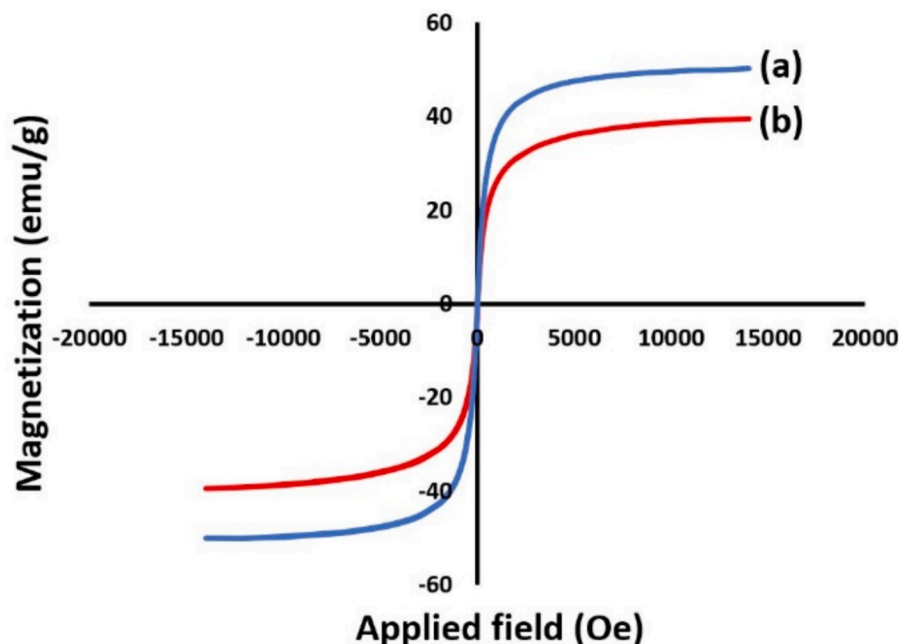


Fig. 8. VSM curves of (a)  $\text{Fe}_3\text{O}_4@\text{COF}$  and (b)  $\text{Fe}_3\text{O}_4@\text{COF-TFA}$ .

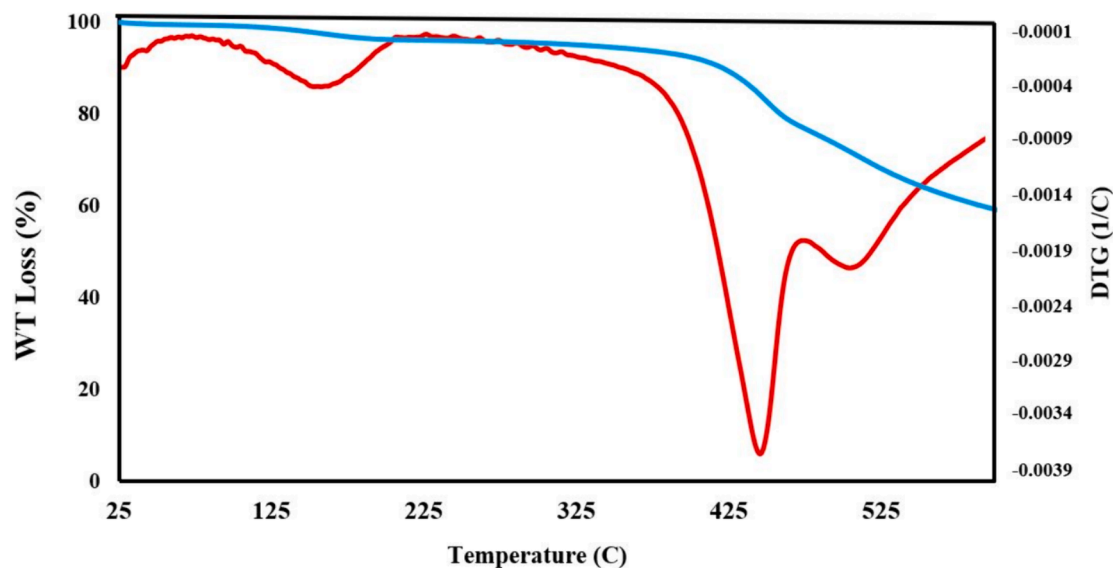


Fig. 9. TGA/DTG curves of  $\text{Fe}_3\text{O}_4@\text{COF-TFA}$ .

illustrated in Fig. 2a-b, which is well in accordance with our expectations. It is worth mentioning that C, N, Fe, and O signals for  $\text{Fe}_3\text{O}_4@\text{COF}$  and C, N, Fe, O and F signals for  $\text{Fe}_3\text{O}_4@\text{COF-TFA}$  can be seen in EDS results which appearance of F signal, in turn, confirms the chemical structure of  $\text{Fe}_3\text{O}_4@\text{COF-TFA}$ . In addition, the uniform distribution of elements in elemental mapping analysis confirmed the EDS results (Figs. 3, 4).

FE-SEM and TEM analysis were used to investigate the morphology of the prepared MCOFs. According to FE-SEM images, the island-like morphologies were illustrated for both  $\text{Fe}_3\text{O}_4@\text{COF}$  (Fig. 5a-b) and  $\text{Fe}_3\text{O}_4@\text{COF-TFA}$  (Fig. 5c-d). Some parts have filamentous morphologies which confirmed the construction of polymeric scaffolds at the surface of  $\text{Fe}_3\text{O}_4$ . Nevertheless, the relatively porous structure for  $\text{Fe}_3\text{O}_4@\text{COF}$  and  $\text{Fe}_3\text{O}_4@\text{COF-TFA}$  was revealed by these images. TEM analysis was applied as proof of FE-SEM images. Accordingly, TEM images show the

spherical geometry for the structure of  $\text{Fe}_3\text{O}_4@\text{COF}$  (Fig. 5e-f) and  $\text{Fe}_3\text{O}_4@\text{COF-TFA}$  (Fig. 5g-h) and the organic layers are well represented at the surface of  $\text{Fe}_3\text{O}_4$ . In addition, TEM images revealed that the size of the magnetic nanoparticles in both  $\text{Fe}_3\text{O}_4@\text{COF}$  and  $\text{Fe}_3\text{O}_4@\text{COF-TFA}$  are in nanometer scale (Fig. 5e-h).

Nitrogen adsorption/desorption isotherms of  $\text{Fe}_3\text{O}_4@\text{COF}$  and  $\text{Fe}_3\text{O}_4@\text{COF-TFA}$  are depicted in Fig. 6. According to these diagrams, the mesoporous structure of the prepared compounds is approved. In addition, the BET surface area of  $\text{Fe}_3\text{O}_4@\text{COF}$  and  $\text{Fe}_3\text{O}_4@\text{COF-TFA}$  are 74 and 12  $\text{m}^2\cdot\text{g}^{-1}$ , respectively. This reduction in the amount of surface area can be attributed to the post-synthetic modification of  $\text{Fe}_3\text{O}_4@\text{COF}$  by trifluoroacetic acid. In addition, The BJH analysis was used to determine the pore size distribution and the results show the pore size distribution for  $\text{Fe}_3\text{O}_4@\text{COF}$  and  $\text{Fe}_3\text{O}_4@\text{COF-TFA}$  mainly lies between 2 to 20 nm and 2 to 60 nm respectively (Fig. 7).

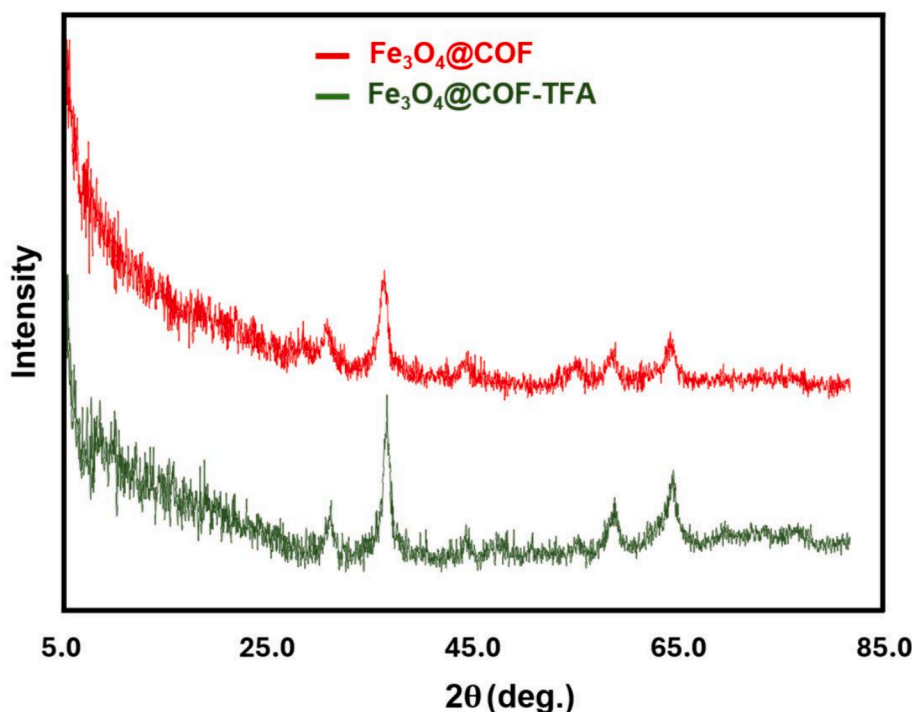
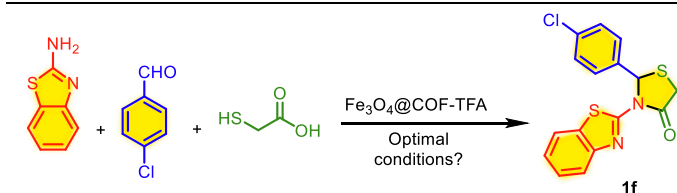


Fig. 10. XRD pattern of  $\text{Fe}_3\text{O}_4@\text{COF}$  and  $\text{Fe}_3\text{O}_4@\text{COF-TFA}$ .

Table 1

Optimizing of the reaction conditions for the synthesis of **1f**<sup>a</sup>.



Entry	Solvent	Catalyst loading (mg)	Temperature (°C)	Time (min.)	Yield <sup>b</sup> (%)	TON	TOF (min <sup>-1</sup> )
1	–	–	90	30	–	–	–
2	–	–	90	60	15	–	–
3	–	5	90	30	45	9000	300
4	–	10	90	30	93	9300	310
5	–	20	90	30	92	4600	153.3
6	–	10	110	30	95	9500	316.6
7	–	10	75	30	80	8000	266.6
8	–	10	50	40	60	4000	100
9	–	10	25	90	–	0	0
10	H <sub>2</sub> O	10	Reflux	30	–	0	0
11	CH <sub>3</sub> OH	10	Reflux	30	45	4500	150
12	C <sub>2</sub> H <sub>5</sub> OH	10	Reflux	30	30	3000	100
13	CH <sub>2</sub> Cl <sub>2</sub>	10	Reflux	30	40	4000	133.3
14	EtOAc	10	Reflux	30	52	5200	173.3
15	<i>n</i> -hexane	10	Reflux	30	–	–	–
16	CHCl <sub>3</sub>	10	Reflux	30	–	–	–

<sup>a</sup> Reaction conditions: 4-chlorobenzaldehyde (1 mmol, 0.14 g), 2-aminobenzothiazole (1 mmol, 0.150), thioglycolic acid (1 mmol, 0.092); <sup>b</sup> Isolated yield.

In another study, the magnetic properties of the prepared MCOFs were measured by using VSM analysis. Both  $\text{Fe}_3\text{O}_4@\text{COF}$  and  $\text{Fe}_3\text{O}_4@\text{COF-TFA}$  have a remarkable magnetization value which are about 50 and 40 emu/g, respectively which guarantees their recovering feasibility by using a suitable external magnet. Nevertheless, the magnetic value of  $\text{Fe}_3\text{O}_4$  is about 70 emu/g (Alishahi et al., 2023) which shows the reduction in the magnetic value of  $\text{Fe}_3\text{O}_4@\text{COF}$  in comparison to  $\text{Fe}_3\text{O}_4$  confirmed the successful addition of organic layers to  $\text{Fe}_3\text{O}_4$  nanoparticles. Also, the diminishing of the magnetic value for  $\text{Fe}_3\text{O}_4@\text{COF}$

TFA is due to the addition of TFA to the supported organic layers on  $\text{Fe}_3\text{O}_4@\text{COF}$  (Fig. 8).

The study of the thermal stability of MCOFs is imperative. Bearing this idea in mind, TG/DTG analysis was used for the evaluation of the thermal stability of  $\text{Fe}_3\text{O}_4@\text{COF-TFA}$ . The analysis was performed from an ambient temperature up to 600 °C under an inert atmosphere. According to TG/DTG curves (Fig. 9),  $\text{Fe}_3\text{O}_4@\text{COF-TFA}$  has excellent thermal stability up to about 450 °C and gradual weight loss up to 165 °C is because of the evaporation of trapped solvents from the pores and

**Table 2**  
Optimizing of the reaction conditions for the synthesis of **2f**<sup>a</sup>.



Entry	Solvent	Temperature (°C)	Catalyst loading (mg)	Time (min.)	Yield (%) <sup>b</sup>	TON	TOF (min <sup>-1</sup> )
1	–	70	10	60	50	5000	83.3
2	–	80	10	60	58	5800	96.6
3	–	90	10	60	62	6200	103.3
4	–	100	10	60	54	5400	90
5	EtOH	70	10	60	70	7000	116.6
6	EtOH	Reflux	10	60	90	9000	150
7	EtOH	Reflux	–	60	50	–	–
8	EtOH	Reflux	20	60	92	4600	76.6
9	EtOH	Reflux	15	60	75	5000	83.3
10	MeOH	Reflux	10	60	65	6500	108.3
11	<i>n</i> -Hexane	Reflux	10	60	30	3000	50
12	EtOAc	Reflux	10	60	40	4000	66.6
13	H <sub>2</sub> O	Reflux	10	60	–	0	0
14	C <sub>2</sub> H <sub>5</sub> OH	Reflux	10	30	trace	0	0

<sup>a</sup> 4-chlorobenzaldehyde (1 mmol, 0.14 g), ethyl cyanoacetate (1 mmol, 0.113 g), malononitrile (1 mmol, 0.066 g) and hydrazine monohydrate (1 mmol, 0.050 g).

<sup>b</sup> Isolated Yields,

surface of Fe<sub>3</sub>O<sub>4</sub>@COF-TFA. The weight loss up to about 40 % before 600 °C confirmed the presence of acceptable amounts of organic layers on the surface of Fe<sub>3</sub>O<sub>4</sub>. According to XRD analysis, although the both Fe<sub>3</sub>O<sub>4</sub>@COF and Fe<sub>3</sub>O<sub>4</sub>@COF-TFA has an amorphous structure, but the diagnostic signals related to Fe<sub>3</sub>O<sub>4</sub> by cubic lattice are at 30°, 35°, 43°, 53°, 57° and 62° confirmed the preservation of the crystalline structure of Fe<sub>3</sub>O<sub>4</sub> (Fig. 10).

The predictable catalytic potential of Fe<sub>3</sub>O<sub>4</sub>@COF-TFA, encouraged us to use it as a heterogeneous catalyst for the construction of the 2,3-disubstituted thiazolidine-4-ones and *N*-amino-2-pyridones via multi-component synthetic route. Hence, we focused on finding the optimal reaction conditions. For this goal, the synthesis of molecule **1f** was used as a model reaction among 2,3-disubstituted thiazolidine-4-ones and several influential parameters such as temperature, solvent and the amounts of the catalyst were explored. The model reaction does not have good progress in the absence of catalyst and only a negligible amount of product was obtained after 60 min. In the following, three amounts of catalyst including 5, 10 and 20 mg were used and according to the results, 10 mg Fe<sub>3</sub>O<sub>4</sub>@COF-TFA was selected as the best amount of catalyst. About optimization of temperature, the model reaction has admirable results at 90 °C compared to lower temperatures. In addition, the role of solvent was markedly studied, and the model reaction was carried out in different polar (protic and aprotic) and nonpolar solvents including H<sub>2</sub>O, MeOH, EtOH, CH<sub>2</sub>Cl<sub>2</sub>, EtOAc, CHCl<sub>3</sub>, and *n*-hexane. Nevertheless, the presence of the solvent did not impressive effect on the progress of reaction and solvent-free conditions were selected as the best conditions. More details can be seen in Table 1. Regarding the synthesis of *N*-amino-2-pyridones, molecule **2f** was selected as a model compound. Unlike the previous reaction, performing the model reaction in the presence of protic solvents such as EtOH and MeOH is more efficient than in solvent-free conditions. Anyway, considering the yield of desired product and green chemistry principles, the best results were obtained by using 10 mg Fe<sub>3</sub>O<sub>4</sub>@COF-TFA as a catalyst in refluxing EtOH (Table 2).

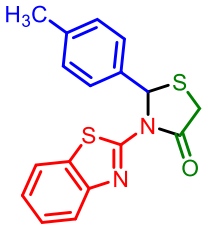
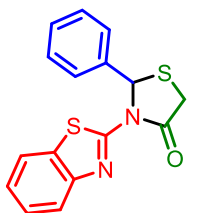
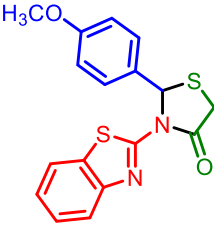
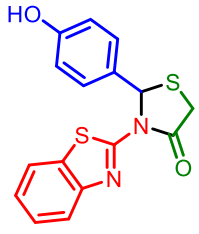
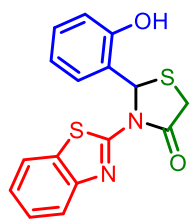
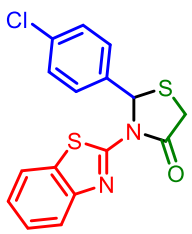
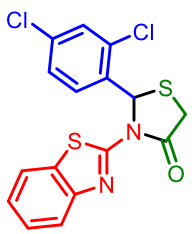
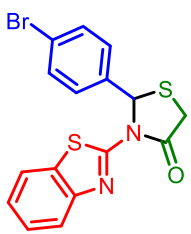
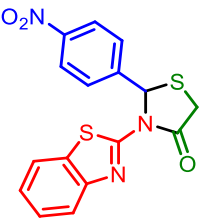
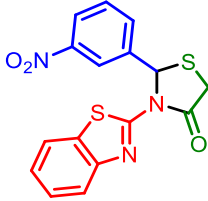
To account for the optimum reaction conditions for the synthesis of 2,3-disubstituted thiazolidine-4-ones and *N*-amino-2-pyridones, the scope and limitations of the reactions were investigated upon using different substituted aryl-aldehydes. Therefore, an assortment of aromatic aldehydes with electron-poor and electron-rich aryl groups and, benzaldehyde was used for the synthesis of the desired molecules. It is worth mentioning that all the achieved molecules have good yields and short reaction times (Table 3, 4). Also, the melting points of the previously reported molecules are embedded in related tables (Kalhor and Banibairami, 2020; Mahapartra and Patanik, 1984; Dolganov et al., 2022).

Also, in a comparative study, we discussed the catalytic activity and efficiency of Fe<sub>3</sub>O<sub>4</sub>@COF-TFA with some of the previously reported procedures for the preparation of **1b** and **2a** compounds. We found that the Fe<sub>3</sub>O<sub>4</sub>@COF-TFA shows a good and acceptable catalytic performance under mild reaction conditions with short reaction time and high yield of product. The recycling and reusing ability of Fe<sub>3</sub>O<sub>4</sub>@COF-TFA is another benefit of this system which this point is not observed in most of the previously reported catalysts (Table 5, 6).

To investigate the key role of the components of this hybrid catalytic system, the **1f** molecule was prepared in the presence of Fe<sub>3</sub>O<sub>4</sub>, Fe<sub>3</sub>O<sub>4</sub>@COF, and TFA compared to Fe<sub>3</sub>O<sub>4</sub>@COF-TFA. The results showed that each of these catalysts can have a catalytic role to some extent. The free hydroxy groups of Fe<sub>3</sub>O<sub>4</sub> have inherent catalytic activity and high specific surface of COF increased the number of effective interactions. Therefore, their synergistic effects with TFA can improve the catalytic potential of Fe<sub>3</sub>O<sub>4</sub>@COF-TFA (Table 7).

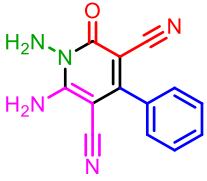
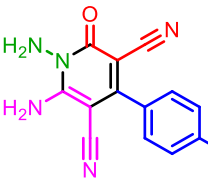
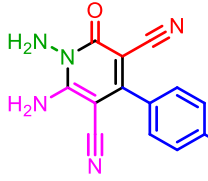
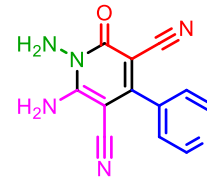
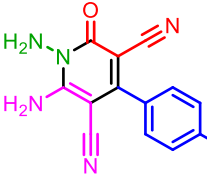
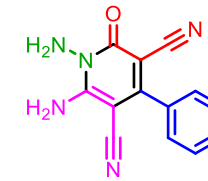
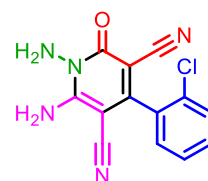
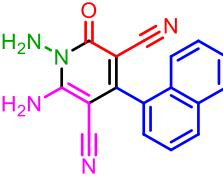
Also, we suggested a plausible mechanistic route for the synthesis of 2,3-disubstituted thiazolidine-4-ones by using Fe<sub>3</sub>O<sub>4</sub>@COF-TFA as a heterogeneous catalyst (Scheme 3). In this mechanism, firstly, the carbonyl group of aryl aldehyde is activated by the catalyst and subjected to a nucleophilic attack reacted from 2-aminobenzothiazole to achieve the intermediate **a**. Then, the reaction of intermediate **a** with thioglycolic acid leads to the formation of intermediate **b**. In the next

**Table 3**  
 Synthesis of 2,3-disubstituted thiazolidine-4-one derivatives in the presence of  $\text{Fe}_3\text{O}_4@\text{COF-TFA}$  as a catalyst.<sup>a</sup>

 <p>1a, 30 min.: 88%        M.p.: 200-201 °C [191-193]<sup>Fazl et al., 2022</sup></p>	 <p>1b, 30 min.: 80%        M.p.: 168-170 °C [172-174]<sup>Fazl et al., 2022</sup></p>	 <p>1c, 25 min.: 80%        M.p.: 159-161 °C [177-178]<sup>Kalhor et al., 2020</sup></p>	 <p>1d, 30 min.: 88%        M.p.: 250-255 °C [210-212]<sup>Mahapartra et al., 1984</sup></p>
 <p>1e, 15 min.: 93%        M.p.: 246-249 °C [248-249]<sup>Fazl et al., 2022</sup></p>	 <p>1f, 30 min.: 93%        M.p.: 197-198 °C [202-204]<sup>Fazl et al., 2022</sup></p>	 <p>1g, 15 min.: 96%        M.p.: 220-222 °C [new]</p>	 <p>1h, 20 min.: 91%        M.p.: 197-200 °C [171-172]<sup>Fazl et al., 2022</sup></p>
 <p>1i, 30 min.: 83%        M.p.: 208-211 °C [172-174]<sup>Fazl et al., 2022</sup></p>		 <p>1j, 30 min.: 80%        M.p.: 163-165 °C [171-172]<sup>Kalhor et al., 2020</sup></p>	

<sup>a</sup> Reaction conditions: Aldehyde (1 mmol), 2-aminobenzothiazole (1 mmol, 0.150 g) and thioglycolic acid (1 mmol, 0.092 g), Solvent-free, 90 °C, catalyst = 10 mg, reported yields are referred to isolated yields.

**Table 4**  
Synthesis of *N*-amino-2-pyridones in the presence of Fe<sub>3</sub>O<sub>4</sub>@COF-TFA as catalyst.<sup>a</sup>

 <p>2a, 60 min.: 90% M.p.:&gt; 300 °C [237-240]<sup>Babaeae et al., 2020</sup></p>	 <p>2b, 50 min.: 89% M.p.:&gt; 300 °C [240-241]<sup>Babaeae et al., 2020</sup></p>	 <p>2c, 70 min.: 92% M.p.:250-252 °C [222-224]<sup>Babaeae et al., 2020</sup></p>	 <p>2d, 80 min.: 80% M.p.:&gt; 300 °C [&gt; 300]<sup>Babaeae et al., 2020</sup></p>
 <p>2e, 75 min.:90% M.p.:&gt; 300 °C [&gt; 300]<sup>Babaeae et al., 2020</sup></p>	 <p>2f, 60 min.:90% M.p.:&gt; 300 °C [&gt; 300]<sup>Babaeae et al., 2020</sup></p>	 <p>2g, 60 min.:88% M.p.: &gt; 300 °C [Not reported]<sup>Dolganov et al., 2022</sup></p>	 <p>2h, 90 min.:80% M.p.:270-273 °C [&gt; 300]<sup>Babaeae et al., 2020</sup></p>
 <p>2i, 90 min.:84% M.p.:&gt;300 °C [New]</p>			

<sup>a</sup> Reaction conditions: Aldehyde (1 mmol), ethyl cyanoacetate (1 mmol, 0.113 g), malononitrile (1 mmol, 0.066 g) and hydrazine monohydrate (1 mmol, 0.050 g), EtOH (10 mL), reflux, catalyst = 10 mg, reported yields are referred to isolated yields.

**Table 5**  
Comparative study of catalytic performance of Fe<sub>3</sub>O<sub>4</sub>@COF-TFA and some of the recent reported papers upon the preparation of **1b**<sup>a</sup>.

Entry	Catalyst	Time	Yield (%)
1	Fe <sub>3</sub> O <sub>4</sub> @COF-TFA (10 mg), solvent-free, 90 °C [this work]	30 min.	80
2	1,4-diethyl-1,4-diazabicyclo[2,2,2]octane-1,4-dium perchlorate (2 mol %), H <sub>2</sub> O, reflux (Pinate and Makone, 2023)	70 min.	88
3	zinc(II) chloride, benzene, reflux (Srivastava et al., 2008)	15 h	72
4	Fe <sub>3</sub> O <sub>4</sub> @SiO <sub>2</sub> /(CH <sub>2</sub> ) <sub>3</sub> -urea-benzoic acid, solvent-free, 80 °C (Fazl et al., 2022)	15 min.	85
5	HClO <sub>4</sub> immobilized on silica, toluene, 100 °C (Kumar et al., 2013)	6 h	70

step, *via* a nucleophilic intermolecular cyclization as well as the removal of H<sub>2</sub>O, the target product is synthesized.

Moreover, we suggested a plausible mechanism for synthesized *N*-amino-2-pyridones. At first, aryl aldehyde is activated by an acidic section of the catalyst and reacts with activated malononitrile which

**Table 6**  
Comparison of catalytic activity of Fe<sub>3</sub>O<sub>4</sub>@COF-TFA and some of recent reported papers upon the preparation of **2a**<sup>a</sup>.

Entry	Catalyst	Time	Yield (%)
1	Fe <sub>3</sub> O <sub>4</sub> @COF-TFA (10 mg), EtOH, reflux [this work]	60 min.	90
2	Piperidine (2 mol%), H <sub>2</sub> O, 20 °C (Hosseini and Bayat, 2018)	12 h	90
3	Potassium fluoride impregnated over alumina EOH/H <sub>2</sub> O, 20 °C (Kshiar et al., 2018)	20 min	87
4	Cobalt sulfide (0.4 mol%), EtOH, reflux (Safaei-Ghomi et al., 2019)	35 min.	88
5	Zinc(II) oxide (8 mol%), EtOH, reflux (Safaei-Ghomi et al., 2014)	40 min.	91
6	Piperidine, EtOH, 80 °C (Ranjbar-Karimi et al., 2018)	50 min.	50

leads to Knoevenagel adduct **a**. Also, hydrazine hydrate reacts by ethyl cyanoacetate, and intermediate **b** is produced. In the next step, due to the reaction of intermediate **b** by intermediate **a**, intermediate **c** is performed. Continuously, intermediate **f** is performed *via* intermolecular

**Table 7**

Exploration of the catalytic activity of Fe<sub>3</sub>O<sub>4</sub>@COF-TFA compared to Fe<sub>3</sub>O<sub>4</sub>, Fe<sub>3</sub>O<sub>4</sub>@COF, and TFA upon the preparation of **1f**<sup>a</sup>

Entry	Catalyst	Load of catalyst	Yield (%)
1	Fe <sub>3</sub> O <sub>4</sub> @COF-TFA	10 mg	93
2	Fe <sub>3</sub> O <sub>4</sub>	10 mg	25
3	Fe <sub>3</sub> O <sub>4</sub> @COF	10 mg	44
4	TFA	10 mol%	50

<sup>a</sup> Reaction conditions: 4-Chloro-benzaldehyde (1 mmol, 0.141 g), 2-amino-benzothiazole (1 mmol, 0.150 g) and thioglycolic acid (1 mmol, 0.092 g), Solvent-free, 90 °C, 30 min.

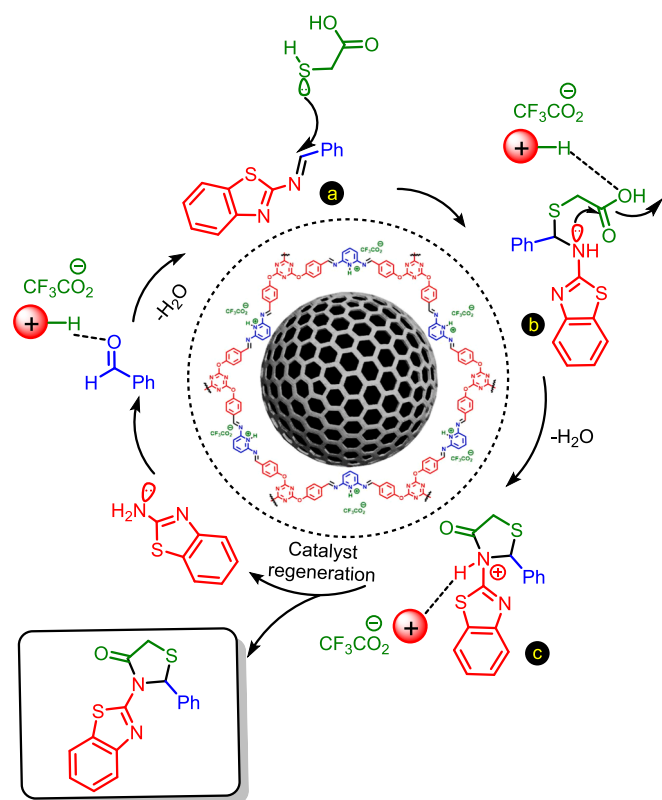
cyclization reaction as well as two tautomerization processes. Finally, the target product is achieved via a cooperative vinylogous anomeric-based oxidation (Alabugin et al., 2021) (Scheme 4).

With this in mind that recovering and reusing ionic catalysts is convenient, one of our goals for the design of Fe<sub>3</sub>O<sub>4</sub>@COF-TFA is its easy recovering and reusing capability. Hence, we delve to the recovery test of Fe<sub>3</sub>O<sub>4</sub>@COF-TFA towards the preparation of desired molecule **1f** under optimal reaction conditions. After completing each run of the model reaction, Fe<sub>3</sub>O<sub>4</sub>@COF-TFA was separated from the mixture of the reaction by using an external magnet and washed with EtOH three times, desiccated, and used in the next run. The results prove that this catalyst can be recovered and reused up to 5 times (Fig. 11). In addition, FESEM and FT-IR analyses were carried out from the recovered catalyst which exhibits that the catalyst has good stability, and its morphology has not changed after running the reaction (ESI).

### 3. Experimental section

#### 3.1. Synthesis of Fe<sub>3</sub>O<sub>4</sub>@COF-TFA

At first, required chemical compounds including Fe<sub>3</sub>O<sub>4</sub> (Torabi et al.,



**Scheme 3.** The suggested mechanistic route for the synthesis of 2,3-disubstituted thiazolidine-4-ones by using Fe<sub>3</sub>O<sub>4</sub>@COF-TFA as a catalyst.

2021) and TFPC (Torabi et al., 2023) were synthesized based on the previously reported methods. The desired products were synthesized according to our recently reported educational synthetic organic method (Zolfigol et al., 2024). In the next step, TFPC (1 mmol, 0.441 g), 2,6-diaminopyridine (1.5 mmol, 0.163 g), Fe<sub>3</sub>O<sub>4</sub> (1 g) and dimethyl sulfoxide (50 mL) were added into a 100 mL flask and sonicated at room temperature for 30 min. After that, 2 mL of acetic acid as a catalyst was added to the flask and heated at 120 °C for 5 h. Then, bulky precipitate was separated by using an external magnet and was washed several times with THF, DCM and MeOH. Then, the precipitate was dried at 100 °C for 12 h. In the next step, Fe<sub>3</sub>O<sub>4</sub>@COF (1 g) was treated with TFA (0.2 mL) in toluene at 60 °C for 12 h and finally washed by EtOH (3 × 20 mL) and dried at 80 °C.

#### 3.2. Preparation of 2,3-disubstituted thiazolidine-4-one derivatives by using Fe<sub>3</sub>O<sub>4</sub>@COF-TFA as a catalyst

Aryl aldehyde derivatives (1 mmol), 2-aminobenzothiazole (1 mmol, 0.150 g), thioglycolic acid (1 mmol, 0.092 g) and Fe<sub>3</sub>O<sub>4</sub>@COF-TFA (0.01 g) were added to the round bottom flask under solvent-free conditions and heated at 90 °C. The progress of the reaction was monitored by using TLC technique. By completing of reaction, the organic compounds were dissolved in DCM (20 mL) while the catalyst is insoluble and was separated by using an external magnet. After that, the DCM was removed and the remained solid was washed by EtOH to yield pure products. Finally, the products were desiccated at 80 °C.

#### 3.3. Preparation of N-amino-2-pyridones derivatives by using Fe<sub>3</sub>O<sub>4</sub>@COF-TFA as a catalyst

In a 10 mL round-bottomed flask, aryl aldehyde (1 mmol), ethyl cyanoacetate (1 mmol, 0.113 g), malononitrile (1 mmol, 0.066 g) and hydrazine monohydrate (1 mmol, 0.050 g), Fe<sub>3</sub>O<sub>4</sub>@COF-TFA (0.01 g) and EtOH (10 mL) were added, and the mixture of reaction was vigorously stirred under reflux conditions. The progress of reactions was checked out by TLC techniques. After completing of reaction, the catalyst was separated from the mixture of the reaction. Then, the solvent was removed and the remained solid was washed by cold EtOH to yield pure products. Finally, the products were desiccated at 80 °C.

#### 3.4. Spectral data

##### 3.4.1. 3-(Benzo[d]thiazol-2-yl)-2-phenylthiazolidine-4-one (1b)

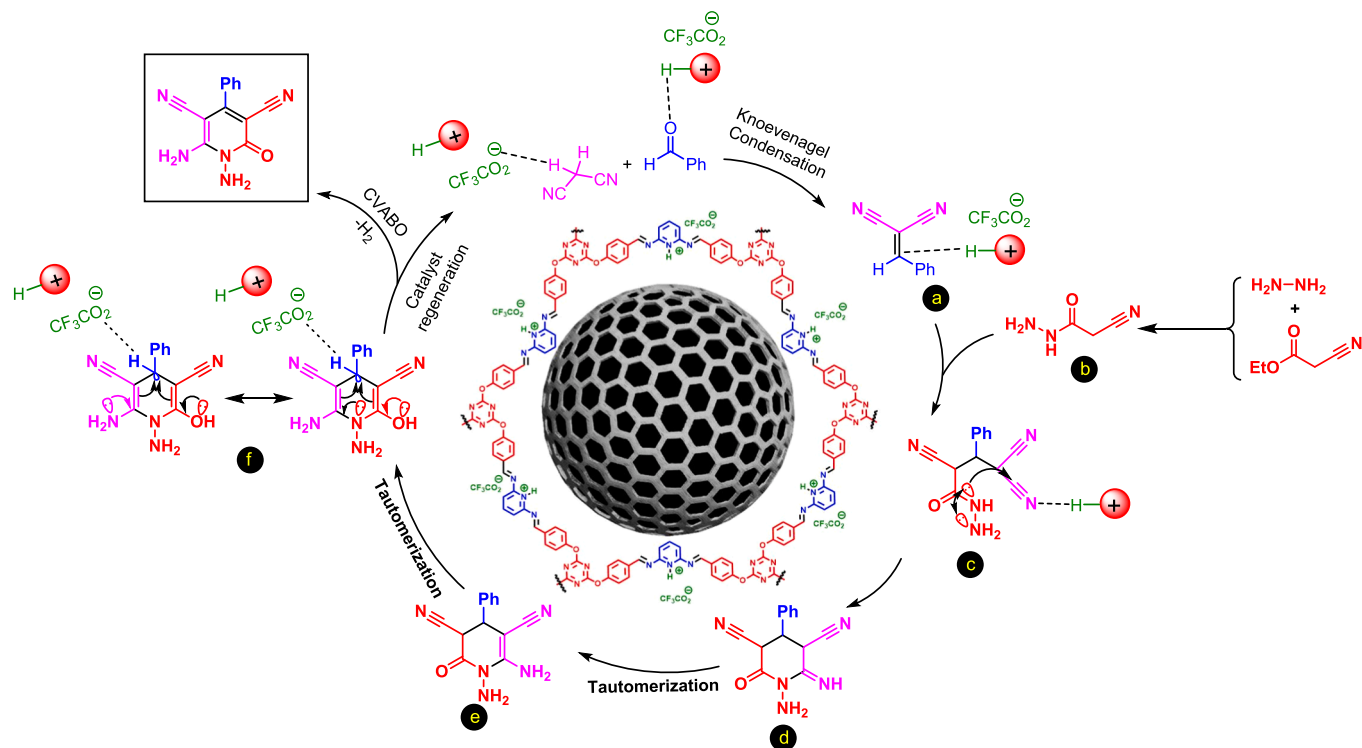
M.p. = 168–170 °C. <sup>1</sup>H NMR (301 MHz, DMSO-d<sub>6</sub>) δ<sub>ppm</sub> 8.06 (d, J=6 Hz, 1H, Aromatic), 7.76 (d, J=3 Hz, 1H, Aromatic), 7.67 (d, J=9 Hz, 1H, Aromatic), 7.46 – 7.34 (m, 5H, Aromatic), 7.21 (d, J=9 Hz, 1H, Aromatic), 6.95 (s, 1H, CH), 4.25 (d, J=15 Hz, 1H, CH), 4.10 (d, J=15 Hz, 1H, CH). <sup>13</sup>C NMR (76 MHz, DMSO-d<sub>6</sub>) δ<sub>ppm</sub> 172.2, 156.4, 148.0, 137.2, 133.8, 132.5, 130.1, 128.4, 126.9, 125.0, 122.5, 121.9, 60.4, 32.2.

##### 3.4.2. 3-(Benzo[d]thiazol-2-yl)-2-(4-methoxyphenyl)thiazolidine-4-one (1c)

M.p. = 159–161 °C, FT-IR (KBr, ν, cm<sup>-1</sup>): 3063, 1697, 1505, 1441, 1375, 758. <sup>1</sup>H NMR (301 MHz, DMSO-d<sub>6</sub>) δ<sub>ppm</sub> 8.04 (d, J=9 Hz, 1H, Aromatic), 7.70 (d, J=9 Hz, 1H, Aromatic), 7.46–7.33 (m, 4H, Aromatic), 6.91 – 6.88 (m, 3H, Aromatic and CH), 4.33 (d, J=15 Hz, 1H, CH), 4.05 (d, J=15 Hz, 1H, CH), 3.72 (s, 3H, CH<sub>3</sub>). <sup>13</sup>C NMR (76 MHz, DMSO-d<sub>6</sub>) δ<sub>ppm</sub> 172.2, 159.4, 156.4, 148.2, 133.5, 131.8, 127.5, 126.8, 124.9, 122.4, 121.8, 63.1, 55.6, 32.4.

##### 3.4.3. 3-(Benzo[d]thiazol-2-yl)-2-(2-hydroxyphenyl)thiazolidine-4-one (1e)

M.p. = 246–249 °C, <sup>1</sup>H NMR (301 MHz, DMSO-d<sub>6</sub>) δ<sub>ppm</sub> 10.17 (s, 1H, OH), 8.04 (s, 1H, Aromatic), 7.68 (s, 1H, Aromatic), 7.38 – 7.35 (m, 2H, Aromatic), 7.12 (s, 1H, Aromatic), 6.95–6.88 (m, 3H, Aromatic), 6.71 (s, 1H, CH), 4.15 (d, J=15 Hz, 1H, CH), 4.3 (d, J=15 Hz, 1H, CH). <sup>13</sup>C NMR



**Scheme 4.** The suggested plausible mechanism for the preparation of *N*-amino-2-pyridones by using  $\text{Fe}_3\text{O}_4@\text{COF-TFA}$  as a catalyst.

(76 MHz,  $\text{DMSO-d}_6$ )  $\delta_{\text{ppm}}$  172.2, 156.4, 148.0, 137.2, 133.8, 132.5, 131.8, 130.1, 128.4, 127.4, 126.9, 125.0, 122.5, 121.9, 60.4, 32.2.

#### 3.4.4. 3-(Benzo[d]thiazol-2-yl)-2-(2,4-dichlorophenyl)thiazolidine-4-one (1 g)

M.p. = 220–222 °C, FT-IR (KBr,  $\nu$ ,  $\text{cm}^{-1}$ ): 2986, 1702, 1508, 1470, 1369, 751.  $^1\text{H}$  NMR (301 MHz,  $\text{DMSO-d}_6$ )  $\delta_{\text{ppm}}$  8.03 (d,  $J=9$  Hz, 1H, Aromatic), 7.68 (d,  $J=9$  Hz, 1H, Aromatic), 7.42–7.24 (m, 5H, Aromatic), 6.94 (s, 1H, CH), 4.31 (d,  $J=15$  Hz, 1H, CH), 4.05 (d,  $J=15$  Hz, 1H, CH).  $^{13}\text{C}$  NMR (76 MHz,  $\text{DMSO-d}_6$ )  $\delta_{\text{ppm}}$  172.2, 156.5, 148.1, 141.6, 131.8, 129.2, 128.5, 126.9, 125.9, 124.9, 122.4, 121.8, 63.2, 32.4.

#### 3.4.5. 3-(Benzo[d]thiazol-2-yl)-2-(4-bromophenyl)thiazolidine-4-one (1 h)

M.p. = 197–200 °C, FT-IR (KBr,  $\nu$ ,  $\text{cm}^{-1}$ ): 2970, 1703, 1508, 1444, 1374, 1444, 761.  $^1\text{H}$  NMR (301 MHz,  $\text{DMSO-d}_6$ )  $\delta_{\text{ppm}}$  8.05 (d,  $J=9$  Hz, 1H, Aromatic), 7.68 (d,  $J=9$  Hz, 1H, Aromatic), 7.56–7.33 (m, 6H, Aromatic), 6.94 (s, 1H, CH), 4.33 (d,  $J=15$  Hz, 1H, CH), 4.06 (d,  $J=15$  Hz, 1H).  $^{13}\text{C}$  NMR (76 MHz,  $\text{DMSO-d}_6$ )  $\delta_{\text{ppm}}$  172.2, 156.5, 148.1, 141.6, 131.8, 129.2, 128.5, 126.8, 125.9, 124.9, 122.4, 121.8, 63.2, 32.4.

#### 3.4.6. 1,6-Diamino-2-oxo-4-phenyl-1,2-dihydropyridine-3,5-dicarbonitrile (2a)

M.p. = > 300 °C, FT-IR (KBr,  $\nu$ ,  $\text{cm}^{-1}$ ): 3455, 3402, 3307, 3253, 2222, 2208, 1643, 1611, 1464.  $^1\text{H}$  NMR (301 MHz,  $\text{DMSO-d}_6$ )  $\delta_{\text{ppm}}$  8.51 (s, 2H,  $\text{NH}_2$ ), 7.86–7.42 (m, 5H, Aromatic), 5.70 (s, 2H,  $\text{NH}_2$ ).  $^{13}\text{C}$  NMR (76 MHz,  $\text{DMSO-d}_6$ )  $\delta_{\text{ppm}}$  160.1, 159.8, 157.2, 135.1, 130.7, 129.1, 128.5, 116.9, 116.0, 86.9, 74.9, 40.8, 40.5, 40.2, 39.9, 39.7, 39.4, 39.1.

#### 3.4.7. 1,6-Diamino-2-oxo-4-(p-tolyl)-1,2-dihydropyridine-3,5-dicarbonitrile (2b)

M.p. = > 300 °C, FT-IR (KBr,  $\nu$ ,  $\text{cm}^{-1}$ ): 3446, 3399, 3307, 3245,

2219, 2206, 1642, 1618, 1599, 1525.  $^1\text{H}$  NMR (301 MHz,  $\text{DMSO-d}_6$ )  $\delta_{\text{ppm}}$  8.48 (s, 2H,  $\text{NH}_2$ ), 7.51–7.18 (m, 4H, Aromatic), 5.68 (s, 2H,  $\text{NH}_2$ ), 2.41 (s, 3H,  $\text{CH}_3$ ).  $^{13}\text{C}$  NMR (76 MHz,  $\text{DMSO-d}_6$ )  $\delta_{\text{ppm}}$  160.1, 159.8, 157.2, 140.6, 132.1, 129.6, 128.5, 117.0, 116.1, 86.8, 74.8, 40.8, 40.5, 40.3, 40.0, 39.7, 39.4, 39.1, 21.5.

#### 3.4.8. 1,6-diamino-4-(2,4-dichlorophenyl)-2-oxo-1,2-dihydropyridine-3,5-dicarbonitrile (2 g)

M.p. = > 300 °C, FT-IR (KBr,  $\nu$ ,  $\text{cm}^{-1}$ ): 3412, 3291, 31943081, 2224, 1671, 1674, 1608, 1568.  $^1\text{H}$  NMR (301 MHz,  $\text{DMSO-d}_6$ )  $\delta_{\text{ppm}}$  8.67 (s, 2H,  $\text{NH}_2$ ), 7.93 (d,  $J=2.0$  Hz, 1H, Aromatic), 7.69–7.66 (m, 1H, Aromatic), 7.59–7.57 (m, 1H, Aromatic), 5.72 (s, 2H,  $\text{NH}_2$ ).  $^{13}\text{C}$  NMR (76 MHz,  $\text{DMSO-d}_6$ )  $\delta_{\text{ppm}}$  159.4, 157.0, 156.8, 136.1, 133.2, 132.4, 131.7, 130.0, 128.6, 116.0, 115.1, 87.5, 75.3, 40.8, 40.5, 40.3, 40.0, 39.7, 39.4, 39.2.

#### 3.4.9. 1,6-diamino-4-(naphthalen-1-yl)-2-oxo-1,2-dihydropyridine-3,5-dicarbonitrile (2i)

M.p. = > 300 °C, FT-IR (KBr,  $\nu$ ,  $\text{cm}^{-1}$ ): 3400, 3325, 3274, 3217, 2217, 1638, 1589, 1523, 1474, 779.  $^1\text{H}$  NMR (301 MHz,  $\text{DMSO-d}_6$ )  $\delta_{\text{ppm}}$  8.56 (s, 2H,  $\text{NH}_2$ ), 8.13–8.07 (m, 2H, Aromatic), 7.75–7.55 (m, 5H, Aromatic), 5.72 (s, 2H,  $\text{NH}_2$ ).  $^{13}\text{C}$  NMR (76 MHz,  $\text{DMSO-d}_6$ )  $\delta_{\text{ppm}}$  159.7, 159.4, 157.1, 133.5, 133.0, 130.4, 129.9, 129.0, 127.8, 127.1, 126.4, 125.9, 124.9, 116.5, 115.6, 88.5, 76.4, 40.8, 40.6, 40.3, 40.0, 39.7, 39.4, 39.2.

## 4. Conclusion

In summary, an ionic containing magnetic COF was successfully synthesized by constructing imine-linked COF on the surface of  $\text{Fe}_3\text{O}_4$  and post-synthetic acidification approach by using TFA. The obtained  $\text{Fe}_3\text{O}_4@\text{COF-TFA}$  was precisely characterized by FT-IR, TGA/DTG, FESEM, EDS, elemental mapping, TEM, VSM and XRD analysis.

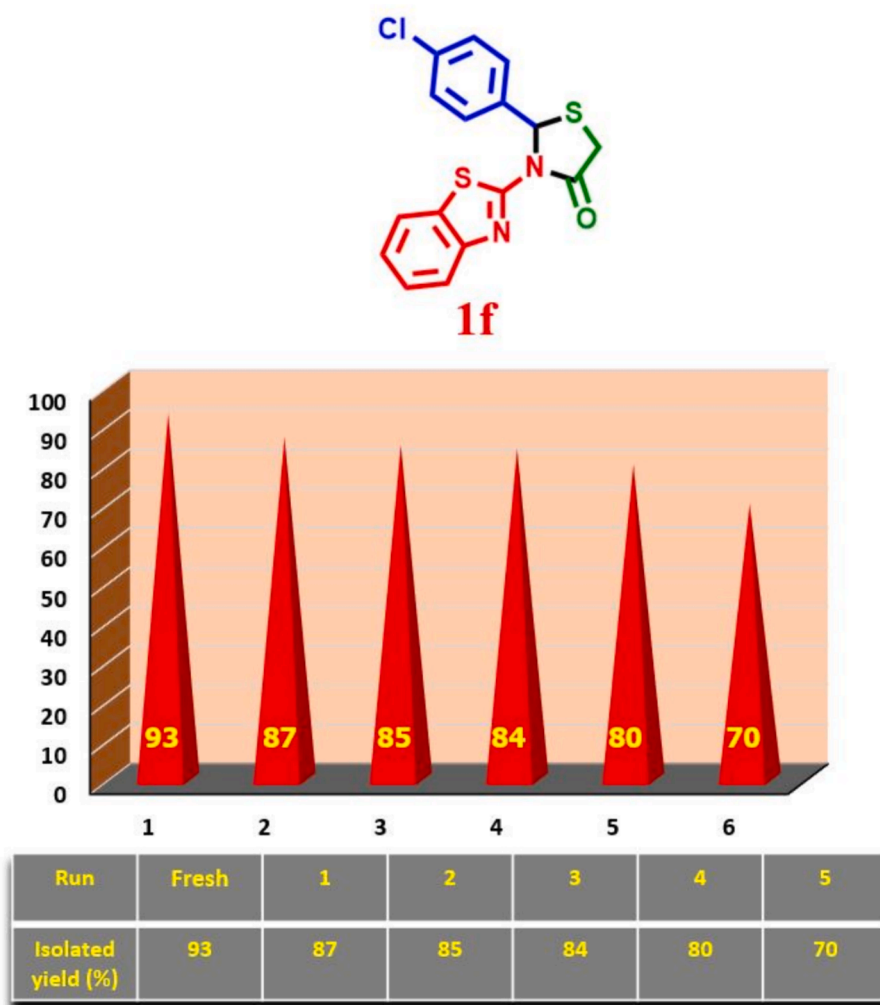


Fig. 11. Recovering and reusing test of  $\text{Fe}_3\text{O}_4\text{@COF-TFA}$  in the synthesis of **1f** under optimum conditions.

$\text{Fe}_3\text{O}_4\text{@COF-TFA}$  due to its porosity and catalytic active sites, exhibit excellent catalytic performance in the multi-component synthesis of 2,3-disubstituted thiazolidine-4-one and *N*-amino-2-pyridone derivatives. The objected multi-component reactions were performed under mild conditions with selectivity and high yield of products. *N*-amino-2-pyridones derivatives were synthesized in EtOH as a green solvent. On the other hand, the recovery and reusability of catalyst as a critical point of ionic catalytic systems were investigated. Accordingly,  $\text{Fe}_3\text{O}_4\text{@COF-TFA}$  was recovered and reused up to 5 times in the synthesis of **1f**. Therefore, this work demonstrates a new approach to the development of COF-based catalysts for many catalytic transformations.

#### CRediT authorship contribution statement

**Erfan Abdoli:** Investigation, Methodology. **Morteza Torabi:** Conceptualization, Investigation, Methodology, Writing – original draft. **Meysam Yarie:** Conceptualization, Investigation, Methodology, Validation, Writing – original draft. **Mohammad Ali Zolfigol:** Conceptualization, Funding acquisition, Project administration, Resources, Supervision, Writing – review & editing.

#### Declaration of competing interest

The authors declare that they have no known competing financial interests or personal relationships that could have appeared to influence the work reported in this paper.

#### Acknowledgments

We thank the Bu-Ali Sina University for financial support to our research group.

#### References

- Abdoli, E., 2023. Catalytic applications of porous organic polymers in  $\text{CO}_2$  fixation. *Iran. J. Catal.* 13, 379.
- Ahadi, E.M., Azizian, H., Vavsari, V.F., Aliahmadi, A., Shahsavari, Z., Bijanzadeh, H.R., Balalae, S., 2021. Synthesis and decarboxylation of functionalized 2-pyridone-3-carboxylic acids and evaluation of their antimicrobial activity and molecular docking. *Iran. J. Pharm. Res.* 20, 456.
- (a) Alabugin, I. V., Kuhn, L., Medvedev, M. G., Krivoshchapov, N. V., Vil, V. A., Yaremenko, I. A., Mehaffy, P., Yarie, M., Terent'ev, A. O., Zolfigol, M. A., 2021. Stereoelectronic power of oxygen in control of chemical reactivity: the anomeric effect is not alone. *Chem. Soc. Rev.* 50, 10253. (b) Alabugin, I.V., Kuhn, L., Krivoshchapov, N.V., Mehaffy, P., Medvedev, M. G. 2021. Anomeric effect, hyperconjugation and electrostatics: Lessons from complexity in a classic stereoelectronic phenomenon. *Chem. Soc. Rev.* 50, 10212. (c) Tavassoli, A., Yarie, M., Torabi, M., Zolfigol, M. A., 2023. Application of novel magnetic *H*-bonding catalyst for synthesis of hybrid pyridine-triazole derivatives bearing indole or sulfonamide segments. *J. Phys. Chem. Solids*, 186, 111786. (d) Zarei, N., Zolfigol, M. A., Torabi, M., Yarie, M., 2023. Synthesis of new hybrid pyridines catalyzed by  $\text{Fe}_3\text{O}_4\text{@SiO}_2\text{@urea}$ -riched ligand/Ch-Cl. *Sci. Rep.* 13, 9486.
- Alishahi, Z., Torabi, M., Zolfigol, M.A., Yarie, M., 2023. Nanoarchitectonics of magnetic covalent organic framework with sulfonic acid tags for catalytic preparation of triazolo quinazolinones and 4H-pyrimidobenzothiazoles. *J. Solid State Chem.* 324, 124119.
- Amer, M.M., Aziz, M.A., Shehab, W.S., Abdellattif, M.H., Mounieir, S.M., 2021. Recent advances in chemistry and pharmacological aspects of 2-pyridone scaffolds. *J. Saudi Chem. Soc.* 25, 101259.

- Anzadeh, M.R., Zolfigol, M.A., Torabi, M., Yarie, M., Notash, B., 2022. Urea-dithiocarbamic acid functionalized magnetic nanoparticles modified with Ch-Cl: Catalytic application for the synthesis of novel hybrid pyridones via cooperative geminal-vinylous anomeric-based oxidation. *J. Mol. Liq.* 364, 120016.
- Ansari, M.A., Yadav, D., Singh, M.S., 2020. Rhodium (II)-catalyzed annulative coupling of  $\beta$ -ketothioamides with  $\alpha$ -diazio compounds: access to highly functionalized thiazolidin-4-ones and thiazolines. *J. Org. Chem.* 85, 8320.
- Babae, S., Zarei, M., Sepehrmansourie, H., Zolfigol, M.A., Rostamnia, S., 2020. Synthesis of metal-organic frameworks MIL-101 (Cr)-NH<sub>2</sub> containing phosphorous acid functional groups: Application for the synthesis of *N*-amino-2-pyridone and pyrano [2, 3-*c*] pyrazole derivatives via a cooperative vinylous anomeric-based oxidation. *ACS Omega* 5, 6240.
- Baharfard, R., Zareyee, D., Allahgholipour, S.L., 2019. Synthesis and characterization of MgO nanoparticles supported on ionic liquid-based periodic mesoporous organosilica (MgO@PMO-IL) as a highly efficient and reusable nanocatalyst for the synthesis of novel spiroindole-furan derivatives. *Appl. Organomet. Chem.* 33, e4805.
- Bai, L., Phua, S.Z.F., Lim, W.Q., Jana, A., Luo, Z., Tham, H.P., Zhao, Y., 2016. Nanoscale covalent organic frameworks as smart carriers for drug delivery. *Chemcomm* 52, 4128.
- Bayatani, M., Torabi, M., Yarie, M., Zolfigol, M.A., Farajzadeh, Z., 2023. Fabrication of an imidazolium-based magnetic ionic porous organic polymer for efficient heterogeneous catalysis of Betti reaction. *J. Mol. Liq.* 390, 122863.
- Cai, M., Li, Y., Liu, Q., Xue, Z., Wang, H., Fan, Y., Li, G., 2019. One-step construction of hydrophobic MOFs@COFs core-shell composites for heterogeneous selective catalysis. *Adv. Sci.* 6, 1802365.
- (a) Cao, S., Li, B., Zhu, R., Pang, H., 2019. Design and synthesis of covalent organic frameworks towards energy and environment fields. *Chem. Eng. J.* 355, 602, (b) Yu, F., Li, C., Li, W., Yu, Z., Xu, Z., Liu, Y., Wang, B., Na, B., Qiu, J., 2024. II-Skeleton tailoring of olefin-linked covalent organic frameworks achieving low exciton binding energy for photo-enhanced uranium extraction from seawater. *Adv. Func. Mater.* 34, 2307230, (c) Wei, T., Sun, C., Guo, X., Zhou, Y., Wang, M., Qiu, X., Wang, Q., Tang, Y., 2024. Petaloid bimetallic metal-organic frameworks derived ZnCo<sub>2</sub>O<sub>4</sub>/ZnO nanosheets enabled intermittent lithiophilic model for dendrite-free lithium metal anode. *J. Colloid Interface Sci.* 664, 596.
- Chen, M., Zhang, J., Liu, C., Li, H., Yang, H., Feng, Y., Zhang, B., 2021. Construction of pyridine-based chiral ionic covalent organic frameworks as a heterogeneous catalyst for promoting asymmetric Henry reactions. *Org. Lett.* 23, 1748.
- Chen, M., Zhou, Y., Ren, S.B., Wang, J., 2022. Methods to make conductive covalent organic frameworks for electrocatalytic applications. *Chinese J. Struct. Chem.* 41, 2212107.
- Dolganov, A.A., Levchenko, A.G., Dahno, P.G., Guz', D.D., Chikava, A.R., Dotsenko, V.V., Aksenova, I.V., 2022. 7-Aryl-3-(hydroxymethyl)-5-oxo-1, 2, 3, 5-tetrahydro [1, 2, 4] triazolo [1, 5-*a*] pyridine-6, 8-dicarbonitriles: Synthesis and predicted biological activity. *Russ. J. Gen. Chem.* 92, 185.
- Fazl, F., Torabi, M., Yarie, M., Zolfigol, M.A., 2022. Synthesis and application of novel urea-benzoic acid functionalized magnetic nanoparticles for the synthesis of 2, 3-disubstituted thiazolidin-4-ones and hexahydroquinolines. *RSC Adv.* 12, 16342.
- Fossa, P., Menozzi, G., Dorigo, P., Floreani, M., Mosti, L., 2003. Synthesis and pharmacological characterization of functionalized 2-pyridones structurally related to the cardiotoxic agent milrinone. *Bioorg. Med. Chem.* 11, 4749.
- Fujii, M., Nishimura, T., Koshiba, T., Yokoshima, S., Fukuyama, T., 2013. 2-Pyridone synthesis using 2-(phenylsulfanyl) acetamide. *Org. Lett.* 15, 232.
- Gao, C., Bai, J., He, Y., Zheng, Q., Ma, W., Lin, Z., 2019. Post-synthetic modification of phenylboronic acid-functionalized magnetic covalent organic frameworks for specific enrichment of *N*-linked glycopeptides. *ACS. Sustain. Chem. Eng.* 7, 18926.
- Geng, K., He, T., Liu, R., Dalapati, S., Tan, K.T., Li, Z., Jiang, D., 2020. Covalent organic frameworks: design, synthesis, and functions. *Chem. Rev.* 120, 8814.
- Ghasemi, P., Yarie, M., Zolfigol, M.A., Taherpour, A.A., Torabi, M., 2020. Ionically tagged magnetic nanoparticles with urea linkers: Application for preparation of 2-aryl-quinoline-4-carboxylic acids via an anomeric-based oxidation mechanism. *ACS Omega* 5, 3207.
- Gloag, L., Mehdipour, M., Chen, D., Tilley, R.D., Gooding, J.J., 2019. Advances in the application of magnetic nanoparticles for sensing. *Adv. Mater.* 31, 1904385.
- Govan, J., Gun'ko, Y.K., 2014. Recent advances in the application of magnetic nanoparticles as a support for homogeneous catalysts. *Nanomater* 4, 222.
- Guo, J., Jiang, D., 2020. Covalent organic frameworks for heterogeneous catalysis: principle, current status, and challenges. *ACS. Cen. Sci.* 6, 869.
- Hernández, F., Sánchez, A., Rendón-Vallejo, P., Millán-Pacheco, C., Alcaraz, Y., Delgado, F., Estrada-Soto, S., 2013. Synthesis, ex vivo and in silico studies of 3-cyano-2-pyridone derivatives with vasorelaxant activity. *Eur. J. Med. Chem.* 70, 669.
- Hernández, F., Sánchez, A., Rendón-Vallejo, P., Millán-Pacheco, C., Alcaraz, Y., Delgado, F., Estrada-Soto, S., 2013. Synthesis, ex vivo and in silico studies of 3-cyano-2-pyridone derivatives with vasorelaxant activity. *Eur. J. Med. Chem.* 70, 669.
- Hosseini, H., Bayat, M., 2018. An efficient and ecofriendly synthesis of highly functionalized pyridones via a one-pot three-component reaction. *RSC Adv.* 8, 27131.
- Hurtado-Rodríguez, D., Salinas-Torres, A., Rojas, H., Becerra, D., Castillo, J.C., 2022. Bioactive 2-pyridone-containing heterocycle syntheses using multicomponent reactions. *RSC Adv.* 12, 35158.
- Jaiswal, V., Mondal, B., Singh, K., Das, D., Saha, J., 2019. [3+ 2]-annulation of azaoxyallyl cations and thiocarbonyls for the assembly of thiazolidin-4-ones. *Org. Lett.* 21, 5848.
- Kalhor, M., Banibairami, S., 2020. Design of a new multi-functional catalytic system Ni/SO<sub>3</sub>H@zeolite-Y for three-component synthesis of *N*-benzo-imidazo-or-thiazole-1,3-thiazolidinones. *RSC Adv.* 10, 41410.
- Kandambeth, S., Dey, K., Banerjee, R., 2018. Covalent organic frameworks: chemistry beyond the structure. *J. Am. Chem. Soc.* 141, 1807.
- Keshk, R.M., Garavelli, M., El-Tahawy, M.M., 2021. Synthesis, physicochemical and vibrational spectral properties of 2-pyridone and 2-aminopyridine derivatives: An experimental and theoretical study. *J. Mol. Struct.* 1225, 129136.
- Khaef, S., Zolfigol, M.A., Taherpour, A.A., Yarie, M., 2020. Catalytic application of sulfamic acid-functionalized magnetic Fe<sub>3</sub>O<sub>4</sub> nanoparticles (SA-MNPs) for protection of aromatic carbonyl compounds and alcohols: Experimental and theoretical studies. *RSC Adv.* 10, 44946.
- Khan, S.A., Ali, M., Latif, A., Ahmad, M., Khan, A., Al-Harrasi, A., 2022. Mercaptobenzimidazole-Based 1, 3-thiazolidin-4-ones as antidiabetic agents: Synthesis, in vitro  $\alpha$ -glucosidase inhibition activity, and molecular docking studies. *ACS Omega* 7, 28041.
- Kshiar, B., Shangliang, O.R., Myrboh, B., 2018. A three component one-pot synthesis of *N*-amino-2-pyridone derivatives catalyzed by KF-Al<sub>2</sub>O<sub>3</sub>. *Synth. Commun.* 48, 1816.
- Kumar, D., Sonawane, M., Pujala, B., Jain, V.K., Bhagat, S., Chakraborti, A.K., 2013. Supported protic acid-catalyzed synthesis of 2, 3-disubstituted thiazolidin-4-ones: enhancement of the catalytic potential of protic acid by adsorption on solid supports. *Green Chem.* 15, 2872.
- (a) Ma, Z., Mohapatra, J., Wei, K., Liu, J. P., Sun, S., 2021. Magnetic nanoparticles: Synthesis, anisotropy, and applications. *Chem. Rev.* 123, 3904, (b) Wu, L., Mendoza-Garcia, A., Li, Q., Sun, S., 2016. Organic phase syntheses of magnetic nanoparticles and their applications. *Chem. Rev.* 116, 10473.
- Mahapartra, B. D., Patanik, R. C., 1984. Fungicidal activities and mass spectral studies of some Schiff bases derived from *p*. hydroxy benzaldehyde and their derivatives. *J. Ind. Chem. Soc.* 1061.
- Mokhtary, M., 2016. Recent advances in catalysts immobilized magnetic nanoparticles. *J. Iran. Chem. Soc.* 13, 1827.
- Payra, S., Saha, A., Banerjee, S., 2017. Recent advances on Fe-based magnetic nanoparticles in organic transformations. *J. Nanosci. Nanotechnol.* 17, 4432.
- Pinate, P., Makone, S., 2023. Novel DABCO based acidic ionic liquid as a green protocol for the synthesis of thiazolidin-4-one derivatives and cytotoxic activity evaluation on human breast cancer cell line. *J. Sulphur Chem.* 44, 20.
- Primitivo, L., Sappino, C., De Angelis, M., Righi, F., Iannoni, M., Lucci, G., Righi, G., 2021. Preparation and asymmetric induction evaluation of the first ephedrine-based ligands immobilized on magnetic nanoparticles. *ACS Omega* 6, 35641.
- Qiu, J., Wang, H., Zhao, Y., Guan, P., Li, Z., Zhang, H., Wang, J., 2020. Hierarchically porous covalent organic frameworks assembled in ionic liquids for highly effective catalysis of C-C coupling reactions. *Green Chem.* 22, 2605.
- Ranjbar-Karimi, R., Darehkordi, A., Bahadornia, F., Poorfreidoni, A., 2018. Dipyrido [1, 2-*b*: 3', 4'-*e*] [1, 2, 4] triazine scaffolds from pentafluoropyridine. *J. Heterocycl. Chem.* 55, 2516.
- Safaei-Ghomi, J., Saberi-Moghadam, M.R., Shahbazi-Alavi, H., Asgari-Kheirabadi, M., 2014. An efficient method for the synthesis of *N*-amino-2-pyridones using reusable catalyst ZnO nanoparticles. *J. Chem. Res.* 38, 583.
- Safaei-Ghomi, J., Esmaili, S., Teymuri, R., Shahbazi-Alavi, H., 2019. Nano-Co<sub>3</sub>S<sub>4</sub> as a retrievable and robust catalyst for the synthesis of 2-oxo-pyridines and 5-oxo-[1, 2, 4] triazolo [2, 3-*a*] pyridines. *Org. Prep. Proced. Int.* 51, 388.
- Sangwan, S., Yadav, N., Kumar, R., Chauhan, S., Dhanda, V., Wallia, P., Duhan, A., 2022. A score years' update in the synthesis and biological evaluation of medicinally important 2-pyridones. *Eur. J. Med. Chem.* 232, 114199.
- Segura, J.L., Royuela, S., Ramos, M.M., 2019. Post-synthetic modification of covalent organic frameworks. *Chem. Soc. Rev.* 48, 3903.
- Shaikh, M.N., Zahir, M.H., 2022. Pd complex of ferrocenylphosphine supported on magnetic nanoparticles: A highly reusable catalyst for transfer hydrogenation and coupling reactions. *J. Organomet. Chem.* 973, 122395.
- Sharma, R.K., Yadav, P., Yadav, M., Gupta, R., Rana, P., Srivastava, A., Gawande, M.B., 2020. Recent development of covalent organic frameworks (COFs): synthesis and catalytic (organic-electro-photo) applications. *Mater. Horiz.* 7, 411-454.
- Sobhanradkani, S., Jafari, A., Zandipak, R., Meidanchi, A., 2018. Removal of heavy metal (Hg (II) and Cr (VI)) ions from aqueous solutions using Fe<sub>2</sub>O<sub>3</sub>@SiO<sub>2</sub> thin films as a novel adsorbent. *Process. Saf. Environment. Protect.* 120, 348.
- Srivastava, A., Singh, P., Gupta, M., Ansari, M.S., Mandhani, A., Kapoor, R., Kumar, A., Dubey, D., 2008. Laparoscopic pyeloplasty with concomitant pyelolithotomy—is it an effective mode of treatment? *Urol. Int.* 80, 306.
- Tan, K.T., Ghosh, S., Wang, Z., Wen, F., Rodríguez-San-Miguel, D., Feng, J., Jiang, D., 2023. Covalent organic frameworks. *Nat. Rev. Methods Primers.* 3, 1.
- Tavassoli, A.M., Zolfigol, M.A., Yarie, M., 2023. Application of new multi-*H*-bond catalyst for the preparation of substituted pyridines via a cooperative vinylous anomeric-based oxidation. *Res. Chem. Intermed.* 49, 679.
- Tawfeek, H.N., Hassan, A.A., Bräse, S., Nieger, M., Mostafa, Y.A., Gomaa, H.A., El-Shreef, E.M., 2022. Design, synthesis, crystal structures and biological evaluation of some 1, 3-thiazolidin-4-ones as dual CDK2/EGFR potent inhibitors with potential apoptotic antiproliferative effects. *Arab. J. Chem.* 15, 104280.
- Torabi, M., 2021. Catalytic applications of porous organic polymers. *Iran. J. Catal.* 11, 417.
- Torabi, M., Yarie, M., Zolfigol, M.A., Azizian, S., 2020. Magnetic phosphonium ionic liquid: Application as a novel dual role acidic catalyst for synthesis of 2'-aminobenzothiazolomethylnaphthols and amidoalkyl naphthols. *Res. Chem. Intermed.* 46, 891.
- Torabi, M., Zolfigol, M.A., Yarie, M., Notash, B., Azizian, S., Azandaryani, M.M., 2021. Synthesis of triarylpyridines with sulfonate and sulfonamide moieties via a cooperative vinylous anomeric-based oxidation. *Sci. Rep.* 11, 16846.
- Torabi, M., Yarie, M., Zolfigol, M.A., Azizian, S., Gu, Y., 2022. A magnetic porous organic polymer: catalytic application in the synthesis of hybrid pyridines with indole, triazole and sulfonamide moieties. *RSC Adv.* 12, 8804.

- Torabi, M., Zolfigol, M.A., Yarie, M., 2023. Construction of a new 2D coral-like covalent organic framework as CuI nanoparticles carrier for the preparation of diverse triazoles. *Arab. J. Chem.* 16, 105090.
- Waller, P.J., Gándara, F., Yaghi, O.M., 2015. Chemistry of covalent organic frameworks. *Acc. Chem. Res.* 48, 3053.
- Wang, W., Liu, C., Zhang, M., Zhang, C., Cao, L., Zhang, C., Chen, S., 2022. In situ synthesis of 2D/2D MXene-COF heterostructure anchored with Ag nanoparticles for enhancing Schottky photocatalytic antibacterial efficiency under visible light. *J. Colloid. Interface. Sci.* 608, 735.
- Wang, Z., Zhang, S., Chen, Y., Zhang, Z., Ma, S., 2020. Covalent organic frameworks for separation applications. *Chem. Soc. Rev.* 49, 708.
- Wu, C., Liu, Y., Liu, H., Duan, C., Pan, Q., Zhu, J., Zhao, Y., 2018. Highly conjugated three-dimensional covalent organic frameworks based on spirobifluorene for perovskite solar cell enhancement. *J. Am. Chem. Soc.* 140, 10016.
- Yang, Y., Börjesson, K., 2022. Electroactive covalent organic frameworks: a new choice for organic electronics. *Trends. Chem.* 4, 60.
- Yang, F., Li, Y., Zhang, T., Zhao, Z., Xing, G., Chen, L., 2020. Docking site modulation of isostructural covalent organic frameworks for CO<sub>2</sub> fixation. *Chem. Eur. J.* 26, 4510.
- Yang, Q., Luo, M., Liu, K., Cao, H., Yan, H., 2020. Covalent organic frameworks for photocatalytic applications. *Appl. Catal. B* 276, 119174.
- Yao, B.J., Wu, W.X., Ding, L.G., Dong, Y.B., 2021. Sulfonic acid and ionic liquid functionalized covalent organic framework for efficient catalysis of the Biginelli reaction. *J. Org. Chem.* 86, 3024.
- Yarie, M., 2021. Spotlight: COFs as catalyst in organic methodologies. *Iran. J. Catal.* 11, 89.
- Yusran, Y., Li, H., Guan, X., Fang, Q., Qiu, S., 2020. Covalent organic frameworks for catalysis. *Energy. Chem.* 2, 100035.
- Zandipak, R., Sobhanardakani, S., 2018. Novel mesoporous Fe<sub>3</sub>O<sub>4</sub>/SiO<sub>2</sub>/CTAB-SiO<sub>2</sub> as an effective adsorbent for the removal of amoxicillin and tetracycline from water. *Clean Technol. Environ. Policy* 20, 871.
- Zarei, N., Torabi, M., Yarie, M., Zolfigol, M.A., 2023. Novel urea-functionalized magnetic nanoparticles as a heterogeneous hydrogen bonding catalyst for the synthesis of new 2-hydroxy pyridines. *Pahs.* 43, 3072.
- Zhang, C., Li, W., Liu, C., Zhang, C., Cao, L., Kong, D., Chen, S., 2022. Effect of covalent organic framework modified graphene oxide on anticorrosion and self-healing properties of epoxy resin coatings. *J. Colloid. Interface. Sci.* 608, 1025.
- Zhang, X., Sun, L., Xu, S., Shao, X., Li, Z., Ding, D., Zhan, P., 2022. Design, synthesis, and mechanistic study of 2-pyridone-bearing phenylalanine derivatives as novel HIV capsid modulators. *Molecules* 27, 7640.
- Zhao, Q., Chen, S., Ren, H., Chen, C., Yang, W., 2021. Ruthenium nanoparticles confined in covalent organic framework/reduced graphene oxide as electrocatalyst toward hydrogen evolution reaction in alkaline media. *Ind. Eng. Chem. Res.* 60, 11070.
- Zhao, G., Qin, N., Pan, A., Wu, X., Peng, C., Ke, F., Zhu, J., 2019. Magnetic nanoparticles@ metal-organic framework composites as sustainable environment adsorbents. *J. Nanomater.* 2019, 1454358.
- Zhuang, S., Wang, J., 2021. Magnetic COFs as catalyst for Fenton-like degradation of sulfamethazine. *Chemosphere* 264, 128561.
- Zhuang, S., Chen, R., Liu, Y., Wang, J., 2020. Magnetic COFs for the adsorptive removal of diclofenac and sulfamethazine from aqueous solution: Adsorption kinetics, isotherms study and DFT calculation. *J. Hazard. Mater.* 385, 121596.
- Zolfigol, M.A., Azizian, S., Torabi, M., Yarie, M., Notash, B., 2024. The importance of non-stoichiometric ratio of reactants in organic synthesis. *J. Chem. Edu.* 101, 877.